Technical Report No. TRL-109

AN EXPERIMENTAL STUDY OF THE AXISYMMETRIC TURBULENT BUOYANT PLUME

by

Mahmood Ahmad

A thesis submitted to the Faculty
of the Graduate School of State University
of New York at Buffalo in partial fulfillment
of the requirements for the degree of
Master of Science

May 1980

ACKNOWLEDGEMENTS

This experimental research was carried out in Parker Engineering Building of State University of New York at Buffalo under the supervision of Dr. William K. George, Professor of Mechanical Engineering. I wish to express my heartiest gratitude to him for the opportunity to initiate this project and for his advice and guidance whenever it was needed. His physical presence during some part of the experiment, even at late nights, is highly appreciated.

I would also like to thank Dr. P. Beuther and S. Capp for their help in setting up the experiment and in assisting me in learning the required techniques. I am also highly grateful to Mrs. Eileen Graber for typing the manuscript on very short notice and for her many contributions to a pleasant working environment.

I am grateful to the Atmospheric Science Division, National Science Foundation for funding the research under grants No. ATM 7601257 and ATM 7923729 and to the government of Pakistan for providing me the opportunity for graduate studies in the U.S.A.

These acknowledgements would be incomplete without the patience and encouragement of my wife and my parents which is greatly appreciated.

TABLE OF CONTENTS

List of Figures

Nomenclature

d	Diameter of the hot-wire sensor
D	Diameter of the nozzle
E_T	Output voltage of the Temperature Anemometer
e_T	Fluctuating part of E_T
E_u	Output voltage of the Velocity Anemometer
e_u	Fluctuating part of E_u
F_o	Buoyancy
$f(n)$	Similarity function for the mean axial velocity
G	Amplifier gain
g	Acceleration due to gravity
$h(n)$	Similarity function for Reynolds stress
I	Current through hot-wire
K	Thermal conductivity
$k(n)$	Similarity function for the radial velocity
L	Forced length scale
ℓ	Hot-wire length
M	Momentum
Nu	Nusselt number
$p(n)$	Similarity function for the mean temperature difference
Q	Flowrate
$q(n)$	Similarity function for the radial turbulent heat flux
Re	Reynolds number
R_w	Resistance of the hot-wire sensor
r	radial coordinate
T	Local temperature
T_f	Film temperature

Nomenclature (cont.)

T_w	Temperature of the hot-wire sensor
T_∞	Ambient temperature
ΔT	Local and ambient temperature difference
t	Temperature Fluctuations
U	Mean axial velocity
u	Axial velocity fluctuations
V	Mean radial velocity
v	Radial velocity fluctuations
X	Axial coordinate
β	Coefficient of thermal expansion
ξ	Dimensionless length
η	Dimensionless radial coordinate
ν	Kinematic viscosity
ρ	Density
ρ_∞	Ambient air density
$\Delta\rho$	Local and ambient density difference
τ	Time

ABSTRACT

The purpose of this investigation is to study the plume experimentally in a uniform environment and to compare the results of measurements with those of other researchers, particularly those of George et al. (6) and Beuther et al. (5).

The plume is generated with a Froude number near unity so as to reach the fully developed flow quickly. The ambient temperature is continuously monitored during the experiment.

A two wire probe is used for measuring the temperature and velocity-like signals, and the measurements are taken at vertical locations of 1, 1.5 and 2 meters.

A polynominal relating Reynolds number and Nusselt number is fitted to the velocity calibration data and gives a good collapse of the data for various flow conditions encountered. A new technique is used for the data analysis which utilizes the fact that the fluctuating anemometer voltages are small compared to the mean bridge voltages, allowing higher order terms in an expansion to be neglected. This represents a substantial improvement over older methods (11) which expand in powers of the turbulence intensity, u/U, which is not small over much of the plume.

The profiles of mean and R.M.S. velocities and temperature and their correlations, normalized by similarity variables, are presented. Also the total buoyancy flux and the contribution to that flux by the turbulence are estimated.

Chapter 1 - Introduction

1.1 The Turbulent Buoyant Plume

A turbulent buoyant plume is defined as a turbulent flow from an isolated source driven by buoyancy added continuously at the source. By contrast, the release of a specific amount of buoyancy generates a thermal while a starting plume is generated when a source of buoyancy is initiated and continued. Of the three - plume, thermal and starting plume, only the plume is stationary and lends itself easily to experimental investigation in the laboratory.

The industrial revolution has brought tremendous changes in human life. Apart from many benefits, some of the problems which people, communities and goverments face in today's world result from the air pollution and water contamination arising from disposal of industrial wastes. One must understand the mechanism by which pollutants are dispersed to keep the concentration of pollutants in the environment within permissible limits suitable for healthy living. Hot gas rising from a smoke stack and thermal discharges into rivers are a few examples of plumes.

The knowledge of buoyancy dominated flows is also important in the atmospheric sciences since such flows play an important role in local weather phenomena. An example of such a flow is a cumulus cloud which is similar to the thermal defined above. While simple plumes almost never occur in the atmosphere, an increased understanding of them will contribute directly to our ability to understand the atmospheric flows.

1.2 The Governing Equations for a Turbulent Buoyant Plume

The basic equations of motion in simplified form in cylindrical coordinates with reference to figure (1-1) can be written as:

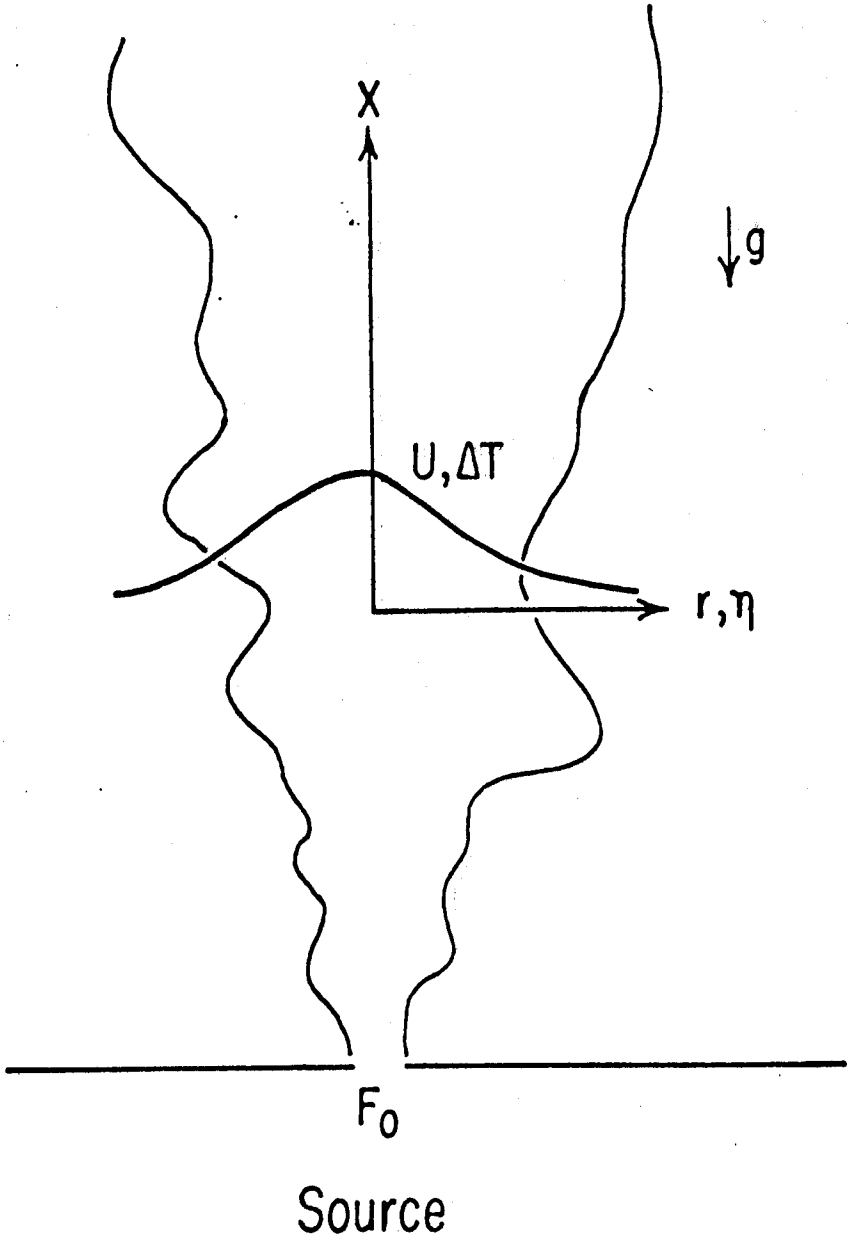

Figure (1-1) Plume Coordinates

Mass Conservation

$$\frac{\partial \bar{U}}{\partial x} + \frac{1}{r}\frac{\partial (r\bar{V})}{\partial r} = 0 \qquad (1.1)$$

Momentum

$$\bar{U}\frac{\partial \bar{U}}{\partial x} + \bar{V}\frac{\partial \bar{U}}{\partial r} + \frac{1}{r}\frac{\partial}{\partial r}(r\overline{uv}) = g\beta\Delta\bar{T} \qquad (1.2)$$

Temperature

$$\bar{U}\frac{\partial (\Delta\bar{T})}{\partial x} + \bar{V}\frac{\partial (\Delta\bar{T})}{\partial r} + \frac{1}{r}\frac{\partial}{\partial r}(r\overline{vt}) = 0 \qquad (1.3)$$

An overbar denotes the average values while lower case letters represent fluctuating quantities. $\Delta\bar{T}$ is the difference between the local mean temperature and the ambient temperature.

The following assumptions have been made in writing these equations;

(i) Statistically stationary flow

(ii) Incompressible flow, except for the buoyancy effect.

(iii) High Reynolds number

(iv) Boussinesq approximation (i.e. deviations from constant density assumed to affect only the buoyancy term).

(v) Streamwise gradient of turbulent normal stress difference has been neglected.

(vi) Streamwise gradient of turbulent heat flux has been neglected.

(vii) Constant pressure field.

For an unstratified (or uniform) environment the plume flow can be characterized by the rate at which buoyancy is added at the source.

defined by

$$F_o = 2\pi \int_0^\infty g\beta(\bar{U}\Delta\bar{T} + \overline{ut})\, z\, dz \tag{1.4}$$

and the x, the distance from the source, since there are no other parameters. In the equation (1-4), the contribution of the streamwise gradient of turbulent heat flux has been included. Zel'dovich (16), Batchelor (3) and Rouse, Yih and Humphrey (12) proposed similarity variables of the form

$$\eta = \frac{z}{x} \tag{1.5}$$

$$\bar{U} = U_s f(\eta) \tag{1.6}$$

$$\bar{V} = U_s h(\eta) \tag{1.7}$$

$$g\beta\Delta\bar{T} = T_s p(\eta) \tag{1.8}$$

$$\overline{uv} = K_s k(\eta) \tag{1.9}$$

$$g\beta\overline{vt} = H_s q(\eta) \tag{1.10}$$

Substituting these relations into the equations of motion, requiring that all terms in the equation have the same x-dependence, and using the integral constraint that F_o to be constant at any section for uniform ambient, we can get

$$\bar{U} = \left[F_o^{1/3} x^{-1/3}\right] f(\eta) \tag{1.11}$$

$$\bar{V} = \left[F_o^{1/3} x^{-1/3}\right] h(\eta) \tag{1.12}$$

$$g\beta\Delta\bar{T} = \left[F_o^{2/3} x^{-5/3}\right] p(\eta) \tag{1.13}$$

$$\overline{uv} = \left[F_o^{2/3} x^{-1}\right] k(\eta) \tag{1.14}$$

$$g\beta\overline{vt} = \left[F_o\, x^{-2}\right] q(\eta) \tag{1.15}$$

Substituting back into the equations of motion results in the following set of similarity equations:

Continuity

$$\eta f' - \frac{1}{3} f + k' + \frac{k}{\eta} = 0 \tag{1.16}$$

Momentum

$$-\eta f f' - \frac{1}{3} f^2 + k f' = \left[-k + \frac{k}{\eta}\right] + p \tag{1.17}$$

Energy

$$-\eta f p' - \frac{5}{3} f p + k p' = -\left[\frac{q}{\eta} + q'\right] \tag{1.18}$$

1.3 History of Theoretical Developments

Turbulent buoyant plumes have been studied theoretically for a number of years. Zel'dovich (10) Rouse et al. (12)and Batchelor (3) independently proposed similarity solutions for plumes, whereas Schmidt (13)and Taylor (14) made assumptions about the basic turbulent flow processes. Morton et al.(9) used an entrainment hypothesis (i.e. radial velocity is proportional to the local mean velocity) to model the turbulent buoyant plume.

Only integral equations were available to model the turbulent buoyant plumes until the mid 1970's when Yih (15)used an eddy viscosity model to get analytical solutions for turbulent Prandtl numbers of 1.1 and 2.0. Later Madni and Pletcher (8) modeled the buoyant jet with a mixing length model. Yih's approach was continued by Hamilton and George (7) and Baker, Taulbee and George (2) who applied it successfully to jets and plumes. Baker et al. presented numerical solutions for a range of Prandtl numbers which agreed with the analytical solutions of Yih for Prandtl numbers of 1.1 and 2.

Very recently Baker (1) has developed a unified theory for buoyant jets and plumes. He has introduced on dimensional and physical grounds a new length scale of the form of $L = M^{3/4}/F_o^{1/2}$ which has been used to non-dimensionalize the axial coordinate to form a new dimensionless length $\xi = \frac{x}{L}$. The dimensionless length ξ controls the buoyancy term in the mean flow momentum equations and hence its evolution from a jet to plume. It has been shown that buoyant jet equations provide plume solutions in the asymptotic region (i.e. for large value of ξ).

1.4 History of Experimental Developments

Most experimental investigations of plumes to date are of a qualitative nature; only few have tried to measure the plume quantitatively. The most cited of these is the experiment by Rouse et al.(12)who used vane anemometers and thermocouples to measure mean velocity and temperature profiles. The empirical data fits for mean velocity and temperature recommended by Rouse et al. are

$$U = 4.7\, F_o^{1/3}\, x^{-1/3} \exp(-96\eta^2) \qquad (1.19)$$

$$g\beta\Delta T = 11 F_0^{2/3} x^{-5/3} \exp(-71\eta^2) \qquad (1.20)$$

where F_0 is the rate at which buoyancy is added at the source and is given by equation (1.4).

Rao and Brzustowski (11) used hot wire anemometers to measure mean and turbulent quantities over burning wicks of various intensities. Unfortunately their data is not presented in a form which can be compared with other available data. They used different overheat ratios at one location to measure mean and fluctuating velocity and, temperature, ant their correlation. Later, George et al. (6) used hot wire anemometers with digital techniques in a turbulent axisymmetric plume to measure the mean and fluctuating quantities, velocity-temperature correlations and the joint probability density of the temperature-velocity fluctuations. Two parallel wires on a single hot wire probe (one being operated at constant temperature and other at constant current) were used to measure temperature and velocity-like signals. George et al.showed that flow is self-preserving; however, the velocity profile did not agree with that of Rouse et al. Velocity and buoyancy profiles were suggested as

$$U = 3.4 F_0^{1/3} x^{-1/3} \exp(-55\eta^2) \qquad (1.21)$$

$$g\beta\Delta T = 9.1 F_0^{2/3} x^{-5/3} \exp(-65\eta^2) \qquad (1.22)$$

Baker et al. later used the form of Yih's analytical solution to obtain a better fit to the data as

$$U = 3.4\, F_0^{1/3}\, x^{-1/3} \left[1 + 28\eta^2\right]^{-2} \tag{1.23}$$

$$g\beta\Delta T = 9.1\, F_0^{2/3}\, x^{-5/3} \left[1 + 28\eta^2\right]^{-3} \tag{1.24}$$

Recently Beuther, Capp and George (4) investigated a stratified plume using a three wire probe in which an x-wire was used to measure two components of velocity and third wire was used for the temperature measurement. Mean velocity and temperature, R.M.S. velocity and temperature, Reynolds stress, axial and radial turbulent heat fluxes,and momentum and energy budgets were calculated from the experimental data. It was found by authors that the mean velocity and temperature profile were best fitted by Yih's eddy viscosity solution and the profiles are given as

$$U = 3.6\, F_0^{1/3}\, x^{-1/3} \left[1 + 33\eta^2\right]^{-2} \tag{1.25}$$

$$g\beta\Delta T = 9.5\, F_0^{2/3}\, x^{-5/3} \left[1 + 33\eta^2\right]^{-3} \tag{1.26}$$

Later measurements by Beuther (4) gave strong indications that the stratification was responsible for the differences with the data of George et al. cited earlier.

1.5 Problems in Previous Work and the Scope of this Thesis.

Only a few people have tried to investigate the plume quantitatively ———— Rouse et al. (12) Nakagome and Hirate (10), Rao and Brzustowsk George et al. (6) and Beuther et al. (5). Results of this limited numbe available experiments do not agree. Moreover even in each experiment, th is sufficient scatter to be quite important. There are a number of possib reasons for the scatter in the data. One reason might be the different

types of instrumentation used in the various experiments. The difficulty of calculating or controlling the amount of the buoyancy added at the source,and the meandering of the plume due to disturbances in the room could be other reasons. Additional factors could involve unwanted thermal stratification and inadvertent modification of the entrainment field. In short the inherent sensitivity of the plume and the complexity of the instrumentation involved are certainly factors which create difficulties.

It was also pointed out by George et al (6) that the scatter in the data of the plume might be due to the fact that measurements were made too close to the source so that the plume is not fully developed. It has been recently shown by Baker (1) that to make sure whether the flow behaves like a plume or jet, the experimentalist should check the dimensionless number $\xi = \frac{x}{L}$. According to this, the flow behaves like a jet if $\xi \leq 1$ and a plume if $\xi \geq 10$.

This work was carried out to specifically address the following question: whether the differences between the results of Beuther (5) and George et al. (6) could be attributed to differences in ambient conditions or experimental techniques. As much as possible the facility, probe and experiment were identical to that of George et al.(6), although the method of data analysis was different.

In the following chapters, the experimental facility and the equipment are described, the calibration technique is outlined, and a new technique for analyzing the temperature dependent velocity signals is introduced. Finally, the experimental results are presented and compared to those of the earlier researchers.

Chapter 2 - Experimental Apparatus and Measurement Techniques

2.1 The Plume Facility

The measurements in turbulent axisymmetric buoyant plume were conducted in the facility located in Parker Engineering Building at the SUNYAB. The plume generator and calibrator is shown in figure (2-1). It consists of a small open jet driven by compressed air and having a section of sintered bronze containing resistive heating elements. There are two screens above the heating elements followed by a contraction of 15:1. Various sections of the generator have been air sealed with gaskets which can withstand a temperature of 1000°F. The nozzle is constructed of aluminum and has been built with the minimum possible amount of material to reduce its thermal capacity and time for stabilization. The entire generator is insulated by several inches of silica gel and contained in a galvanized steel can to reduce the heat loss by conduction.

The axisymmetric plume is produced by taking air from a high pressure tank and passing it through the heater and nozzle. Before being heated the air is passed through a 1 micron filter to absorb moisture and oil, and then through a calibrated flowmeter to measure the mass flow rate. A thermometer is placed in the air line, before the heater and after the flowmeter, to measure the air inlet temperature. With passage of time some oil drops may appear in the flowmeter which may affect the calibration and change the experimental results. Therefore regular cleaning of rotomet is important to maintain good accuracy in calibration.

The SRC power supply connected to resistive elements can raise the exit temperature in excess of 300°C. The exit temperature is maintained to within $\pm$ 1°C of variation for an indefinite period of time and over a wide range of flow conditions by an Electromax Controller which monitors a thermocouple placed at the contraction exit and controls the power supply

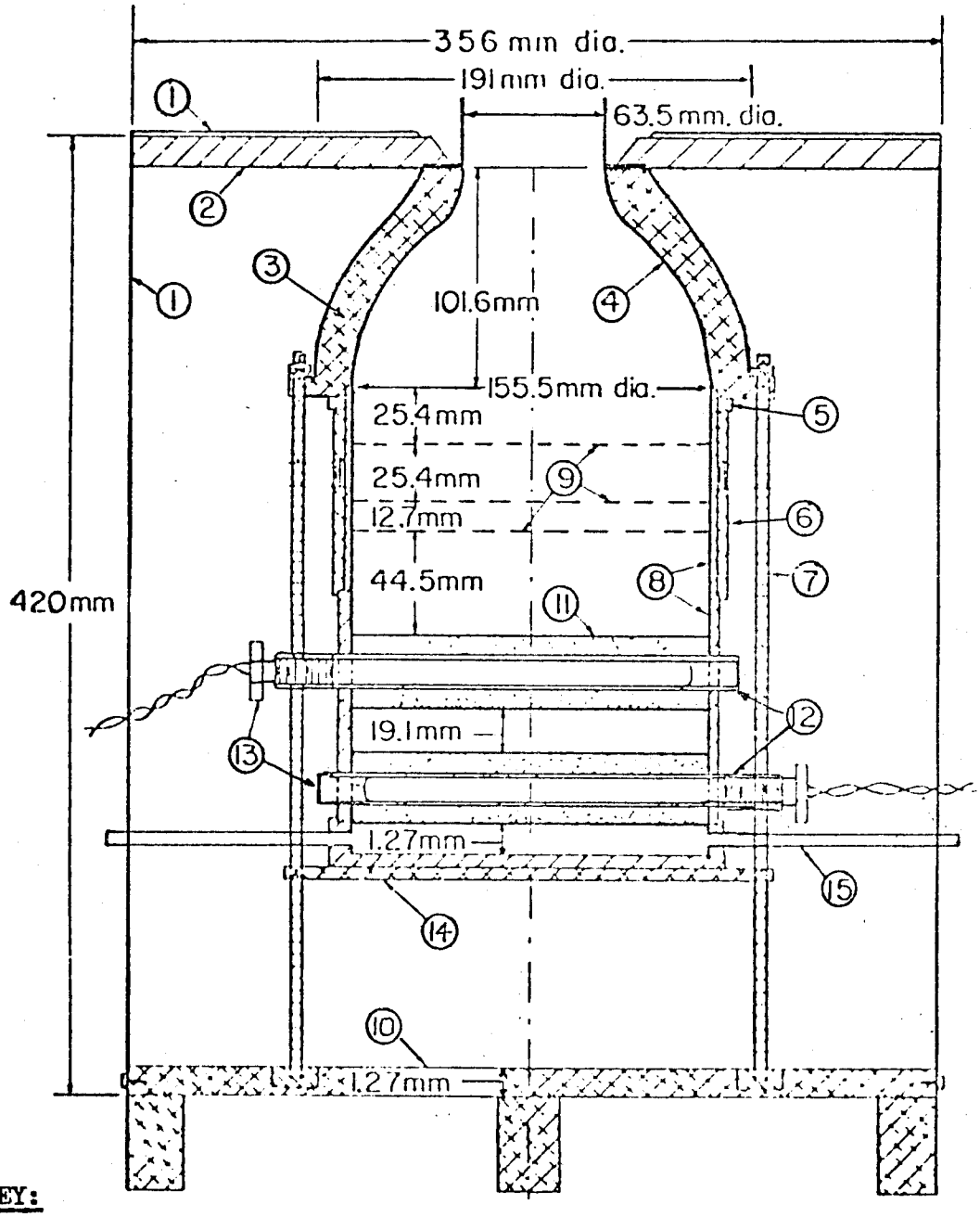

KEY:

(1) Container for silica aerogel insulation, sheet steel. (2) Cerafelt insulation. (3) Aluminum exit nozzle. (4) inner surface; Radius (mm.) = $31.75 + 2.42E{-}08\ x^5 - 6.1E{-}06\ x^4 + 4.36E{-}04\ x^3$. (5) Gasket. (6) Bronze sleeve. (7) Three threaded rods spaced 120° apart. (8) Copper spacer. (9) Stainless steel screens; 1.18 wires/mm.,0.305 mm. dia. (10) Aluminum base plate. (11) Two sintered bronze castings; density 5 g/cm^3, smallest passage 150 um. (12) Eight copper pipes; top four positioned perpendicular to bottom four. (13) Eight electric heaters; Watlow Firerod C6A81, 400 W. each. (14) Bronze base plate. (15) Four air inlet pipes, 90° apart.

Figure (2-2) Plume Calibrator

output. A dial setting of 625 on the Electromax Controller gives an exit temperature of about 297°C.

The plume generator is placed in the center of the base of a large structure 6 x 6 ft. in cross-section and 20 ft. high. The facility is illustrated in figure (2-2). The structure is located in a large room of 24 ft. height and approximately 5,000 sq. ft. in area. Three mesh wire screens of different sizes are provided at three different locations to prevent unwanted circulation. Each screen consists of two layers in thickness. The outermost goes around the structure and extends up to the full height. The middle one of approximately 5 ft. diameter is of octagonal shape and rises to 8 ft. The innermost screen is a circular cylinder 2 ft. in diameter and 15 ft. in height. The top of the plume structure is covered with a plywood sheet having a hole of 4 ft. in diamet which is covered with a screen. (This circular opening has been provided with a hope of keeping the plume centered on the vertical.)*

The whole facility is wrapped by a 4 mil plastic sheet to prevent cross drafts. The distance between the plastic and outer screen is about 6-8 inches. Since survival of the plume is dependent on the supply of fresh air, air is fed into the base of the structure and rises between the plastic and outer screen so that it can be entrained radially in towards the center of the plume. It has been observed very clearly that the gap between the plastic and outer screen is very important for maintaining the plume environment in a neutral state. If this gap is interfered with or closed, there is a continuous change in the ambient temperature and the facility becomes stably stratified. The recognition of this fact represents an important finding of this investigation and will be seen to be primarily responsible for the differences in the work of George

*This was not used in the experiment of Beuther (4) or Beuther et al. (5)

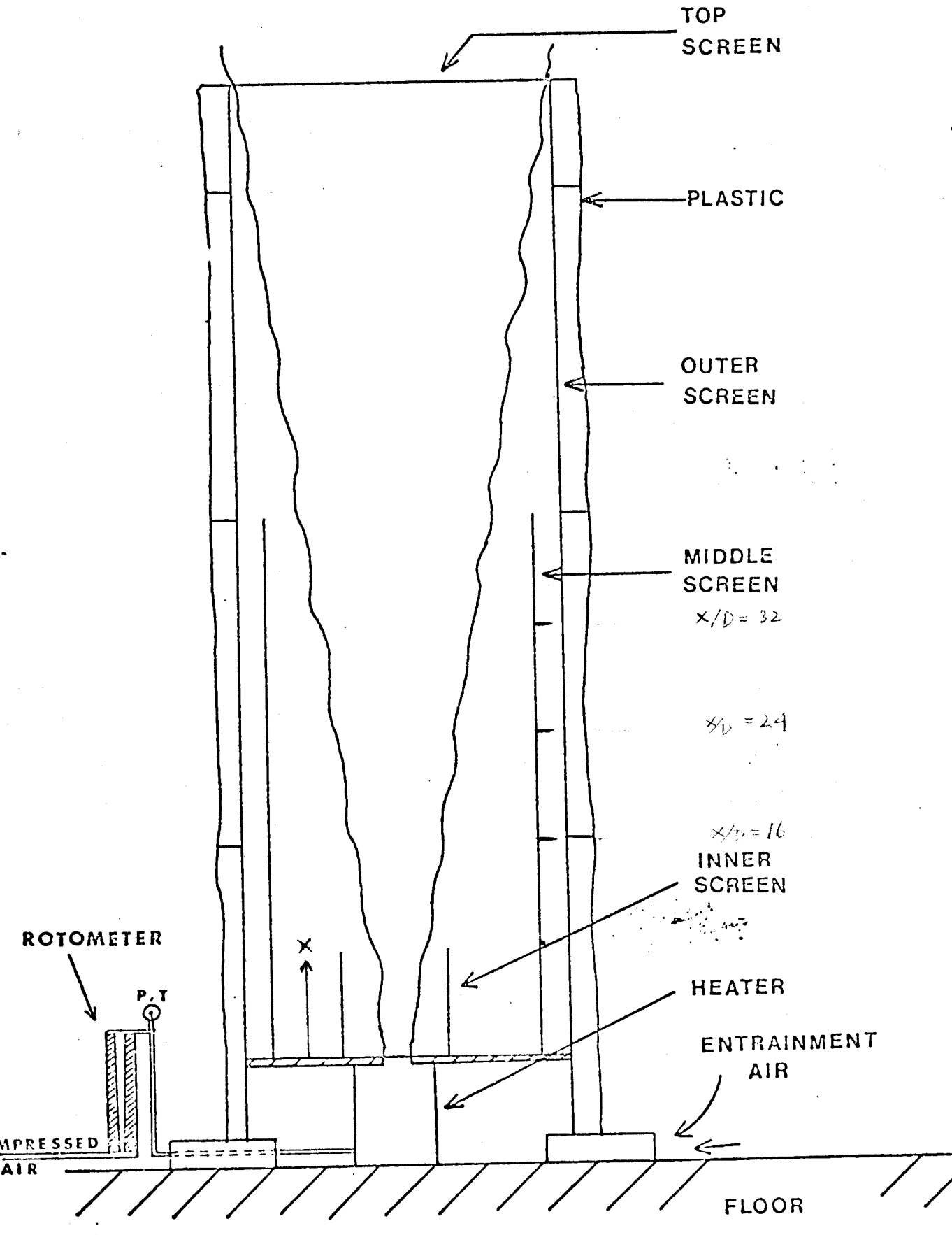

Figure (2-2) Plume Facility

et al. (6) and Beuther (5) referred to earlier. The latter work used the same facility as this investigation but a solid wooden shutter which restricted the fresh air supply was used to separate the plastic from the outer screen.

In this experiment, the ambient temperature was continuously monitored by seven thermocouples fixed at seven different vertical locations, 0.5 m apart.

A traversing mechanism is mounted on one side of the frame and is used to traverse the probe across the plume. It can be placed manually at various heights, 1 meter apart. At one location the probe can travel under manual or computer control over a vertical range of 1 m and across the flow.

2.2 Probe and Anemometers

The hot wire probe used for turbulence measurements is illustrated in figure (2-3). It consists of two parallel wires of 5 micron diameter tungsten with gold plated ends and a length to diameter ratio of 250. The probe (55P76) is designed and manufactured by DISA Electronics. A 90° bent holder (DISA 55H24) was used to hold the probe in position. One wire was used to measure velocity and was operated with an overheat ratio in the range of 1.4-1.6. The other wire operated at much lower overheat and was used as a resistance thermometer. The position of the probe was such that the velocity wire was on top of the temperature wire to avoid the effect of the hot wake on temperature measurement.

Coaxial cables of 5 meters length were used from probe holders to anemometers. Bare connectors on the velocity and temperature cables were insulated to avoid the electrical contact between them. It was noticed that there was an appreciable error in the voltmeter readings due to contact between bare connectors which created a ground loop in the circuit.

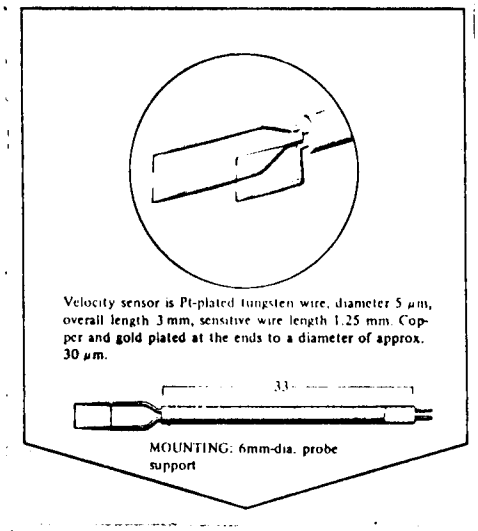

Figure (2-3) Probe

The velocity and temperature wires were connected to the constant temperature anemometer (DISA 55M10) and constant current anemometer (DISA 55M20) respectively to obtain temperature and velocity-like signals. Before operating, the anemometers were stabilized using the built-in square wave generator and observing the anemometer output on the oscilloscope. It was found that in most cases HF = 3 and gain = 5 on the velocity anemometer yielded the optimum condition. This yielded a frequency response for the constant temperature anemometer well above that encountered in this investigation. The cutoff frequency for the constant current wire was estimated by George et al (6) and Beuther (5) to be in excess of 1 KHz, which is also well above that encountered here.

2.3 Experimental Procedure

As both the flow and temperature could be varied independently, it was possible to obtain a source densimetric Froude number near unity resulting in a quick transition to a fully developed plume. The flow rate was kept at 150 ft ^{3}/hr. which remained fairly constant to within $\pm$ 1% during the experiment. The exit temperature of 297°C was constant to within $\pm$ 1° during the test run. These source conditions provided a Froude number near unity.

The plume was turned on for at least four hours before running the experiment, giving enough time for the nozzle and heater walls to reach thermal equilibrium. Measurements were taken at various values of $\eta = r/x$ with a spacing of $\Delta\eta = .025$ between points. Actual values of probe displacement from the center point vary with the height. The experiment was conducted at vertical locations of 1, 1.5, and 2 meters which corresponds to an x/D of 16, 24, and 32 respectively.

The schematic of the apparatus for data acquisition is shown in

figure (2-4). The anemometer bridge output voltages were fed to the integrating digital voltmeter (DISA 55D31) and averaged for 100 seconds to obtain the mean temperature and velocity-like signals. The same two signals were input to the R.M.S. voltmeter (DISA 55D35) via the signal conditioners (DISA 55D26) and averaged for 100 seconds to obtain R.M.S. velocity-like and temperature signals. Because of the low frequencies which characterized this investigation (5-50 Hz), it was necessary to ensemble average successive readings for 10-20 minutes to obtain stable averages (within 5%).

High frequency noise was filtered by passing the signals through the signal conditioners at 1 KHZ low pass. Velocity and temperature signals were added and subtracted before squaring and averaging to obtain the velocity-temperature correlation. The analysis in detail is given in Chapter 3. As two signals were being added and subtracted, it was necessary to keep both the signals in approximately the same order of magnitude. Consequently the velocity signal was amplified by varying the gain from 2-10 depending upon the probe position in the flow. One signal conditioner performed simply as an amplifier and filter. Velocity, temperature and the added and subtracted signals were obtained by changing the function switch on the other signal conditioner.

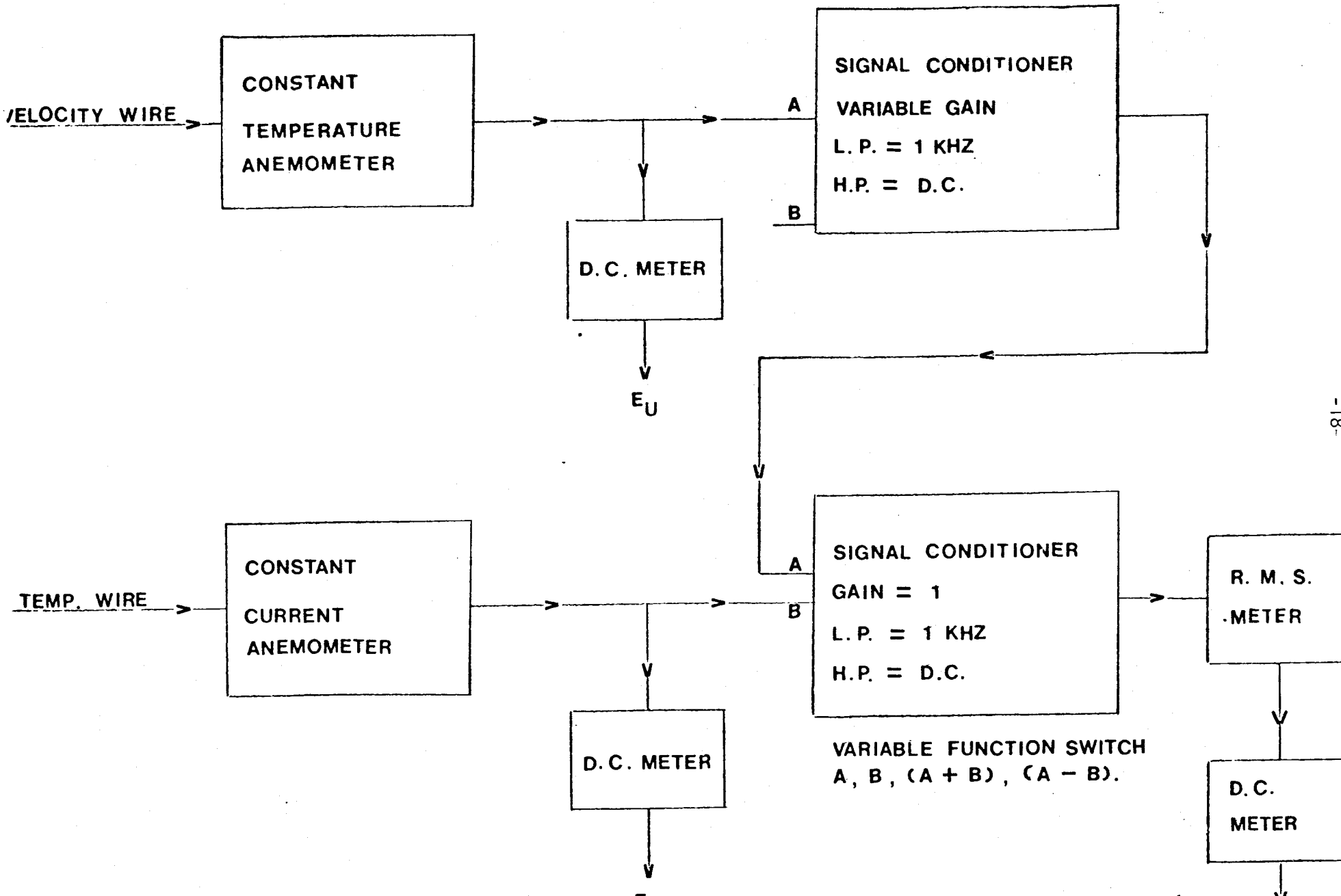
VELOCITY WIRE
CONSTANT
TEMPERATURE
ANEMOMETER
D.C. METER
E_U
A
B
SIGNAL CONDITIONER
VARIABLE GAIN
L.P. = 1 KHZ
H.P. = D.C.
TEMP. WIRE
CONSTANT
CURRENT
ANEMOMETER
D.C. METER
A
B
SIGNAL CONDITIONER
GAIN = 1
L.P. = 1 KHZ
H.P. = D.C.
VARIABLE FUNCTION SWITCH
A, B, (A + B), (A − B).
R.M.S.
METER
D.C.
METER

Chapter 3 - Calibration and Data Processing

3.1 Calibration

Velocity and temperature wire calibration is accomplished simultaneously using the plume generator discussed earlier. The flowmeter measures the flow velocity and a copper-constantan thermocouple placed at the exit gives the temperature. The corresponding velocity and temperature anemometer voltages are read on the DC voltmeters. The flowmeter was calibrated from 50 $ft.^3/hr.$-400 $ft.^3/hr.$ (velocity range range of about 0.1 m/sec. to 1.0 m/sec.)which covers the range of velocities encountered in this investigation. The flow temperature is varied from about 10°C to 52°C which corresponds to the range of flow conditions encountered in the plume.

The calibrating probe is slightly dipped into the nozzle to protect it from cross-drafts, with the result that quite stable readings on the meters are obtained. It is also observed that if the calibration started from lower flowrates and proceeded up, stable readings at lower velocities were possible, whereas considerable fluctuations are encountered at lower velocities if reverse path is followed. This is due to large time constant of the heater at low velocities and the instability introduced by the faster controller.

Computer program WIRCAL converts the flowrates in ft^3/hr and temperature in millivolts into velocity in meters/sec and temperature in ^oK respectively. The velocity wire data is converted to Reynolds (Re) and Nusselt's number (Nu) forms, where these are defined as

$$Re = \frac{U d}{\nu} \tag{3.1}$$

$$Nu = \frac{I^2 R_w}{\pi \ell K_f (T_w - T)} \tag{3.2}$$

where R_w is the resistance of the wire at the operating temperature.

A polynominal of the form of

$$Re = B_0 + B_1 Nu^{1/2} + B_2 Nu + B_3 Nu^{3/2} + B_4 Nu^2 \tag{3.3}$$

gives the best fit to the calibration data in the velocity range considered. The thermal conductivity k_f in the Nusselt number Nu is calculated at the film temperature $T_f = \frac{T_w + T}{2}$. The kinematic viscosity in the Reynolds number Re is calculated at the local flow temperature.

The temperature wire obeys a simple linear law of the form

$$T = A_0 + A_2 E_T \tag{3.4}$$

The velocity wire data conversion into Re number, Nu number form, and the polynominal fit to the data is achieved by running the program "CURFIT". The plot of Re number versus Nu number can be seen on the terminal screen using program "PLX".

Typical temperature and velocity calibration curves are shown in figures (3-1) and (3-2) respectively. It is observed that parameter dR/dt the thermal coefficient of resistivity, used in program "CURFIT" plays a

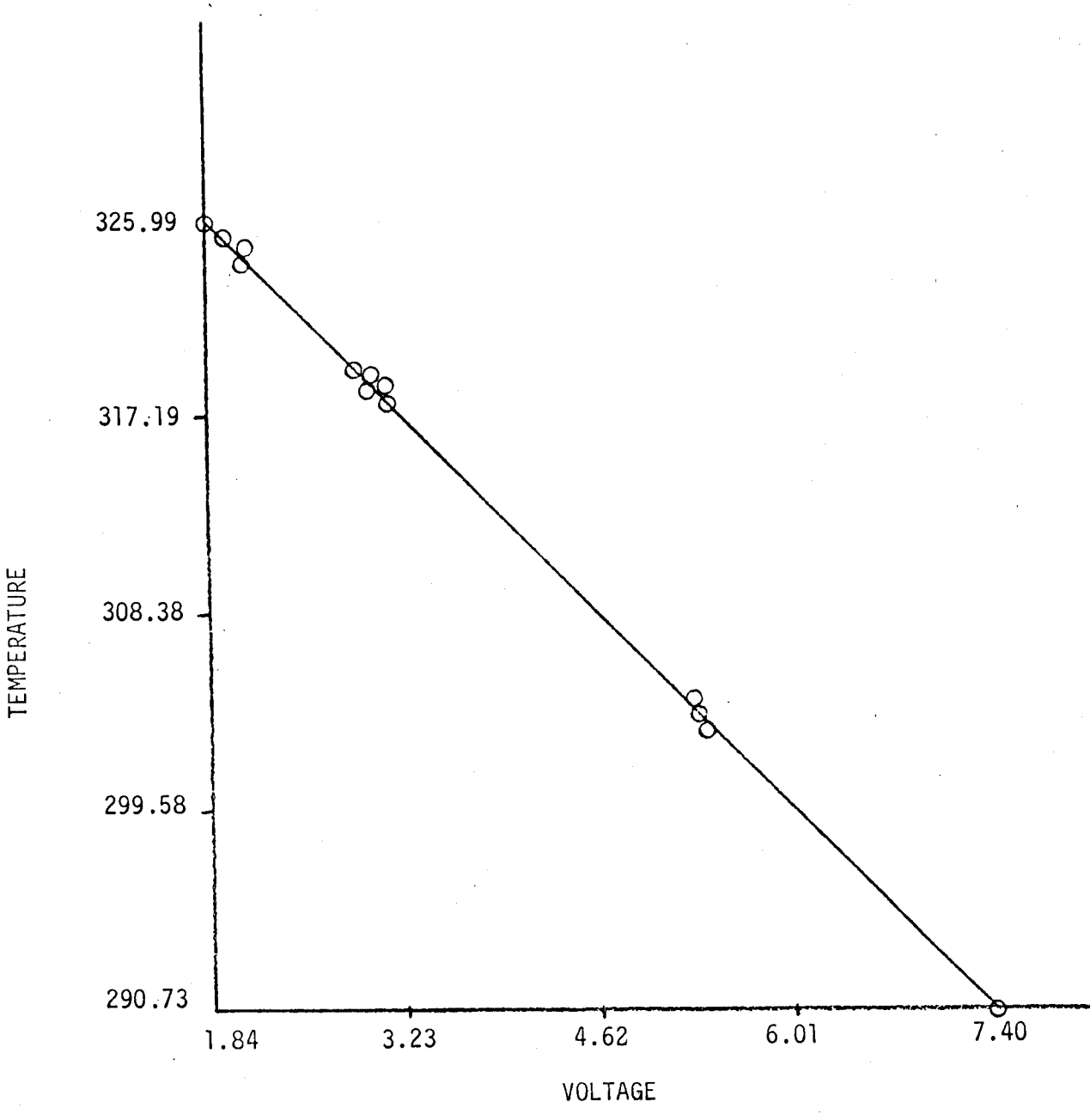

Figure (3-1) Temperature Calibration Data

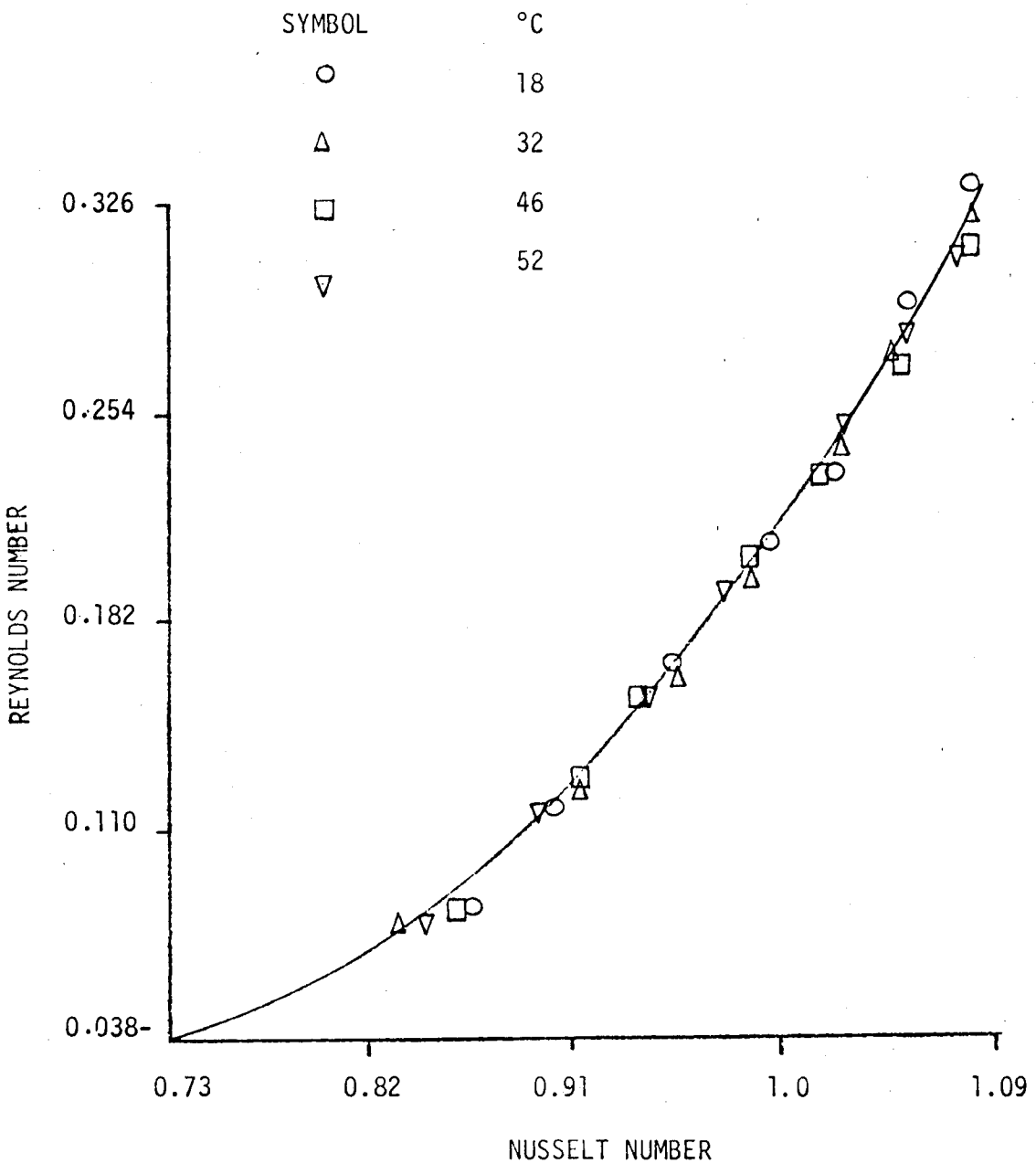

Figure (2-3) Velocity Calibration Data

very important role in collapsing the velocity wire data for various temperatures. It is very difficult to measure exactly the resistance of the wire which is used for precise determination of dR/dT. After curve fitting this parameter is slightly adjusted to collapse the data.

3.2 Data Acquisition

The mean velocity-like and temperature signals (i.e. $\overline{E}_u$ and $\overline{E}_T$) are directly recorded from D.C. voltmeters. R.M.S. velocity-like and temperature signals (i.e. $\sqrt{\overline{e_u^2}}$ and $\sqrt{\overline{e_T^2}}$) are read on R.M.S. meters with a function switch setting at A and B respectively on the second signal conditioner(refer to figure 2-4). Meter readings are divided by the gain setting to obtain actual values.

The velocity-temperature correlation signal $\overline{ut}$, is obtained by addition and subtraction of the two individual signals with the function switch at the (A+B) and (A-B) settings respectively. The correlation is derived as explained below where G_1 and G_2 are the gains for the respective signals.

$$(G_1 A)^2 + (G_2 B)^2 + 2 G_1 G_2 AB = (G_1 A + G_2 B)^2 \tag{3.5}$$

$$(G_1 A)^2 + (G_2 B)^2 - 2 G_1 G_2 AB = (G_1 A - G_2 B)^2 \tag{3.6}$$

Subtracting (3.6) from (3.5) yields the $\overline{AB}$ correlation as

$$\overline{AB} = \frac{(G_1 A + G_2 B)^2 - (G_1 A + G_2 B)^2}{4 G_1 G_2} \tag{3.7}$$

The procedure is illustrated in figure (2-4).

3.3 Data Conversion Equations

Mean Temperature

The mean temperature signals recorded by D.C. voltmeters were converted to the actual temperatures using the linear calibration given in equation (3.4). Decomposing the instantaneous values into mean and fluctuating components and then averaging yields

$$\bar{T} = A_0 + A_2 \bar{E}_T \tag{3.8}$$

where A_0 and A_2 are determined from the calibration data.

R.M.S. Temperature

The R.M.S. temperature is given by

$$\sqrt{t^2} = \lim_{\tau \to \infty} \frac{1}{\tau} \left[\int_0^{\tau} (T - \bar{T})^2 \right]^{1/2} \tag{3.9}$$

Substituting equations (3.4) and (3.8) into equation (3.9) and simplifyin yields

$$\sqrt{t^2} = A_2 \sqrt{e_T^2} \tag{3.10}$$

Mean Velocity

The velocity calibration relation in non-dimensionalized and temperature independent form is given in equation (3.3) where the constants are determined from the calibration data. The equation (3.3) can be subjecte to the Reynolds decomposition method to find the actual mean velocity at any location in the flow from the recorded velocity-like signals. Averaging yields

$$\bar{Re} = B_0 + B_1 \overline{Nu^{1/2}} + B_2 \overline{Nu} + B_3 \overline{Nu^{3/2}} + B_4 \overline{Nu^2} \tag{3.11}$$

Consider each term on the right hand side of equation (3.11) individually. From equation (3.2), the Nusselt number can be written as

$$Nu = \frac{E_u^2 R_w}{(R_w + 51)^2 \pi \ell (T_w - T) K} \tag{3.12}$$

where $(R_w + 51)$ is the sum of the resistances of the active arm of the bridge and resistance of the wire at the operating temperature. Equation (3.12) can be rewritten as

$$Nu = \frac{C_1 E_u^2}{K (T_w - T)} \tag{3.13}$$

where

$$C_1 = \frac{R_w}{(R_w + 51)^2 \pi \ell} \tag{3.14}$$

Substitution of equation (3.4) into equation (3.13) and letting $T_w - A_o = C_2$ and $A_2 = C_3$ we get

$$Nu = \frac{C_1 E_u^2}{K (C_2 - C_3 E_T)} \tag{3.15}$$

The velocity-like and temperature voltages can be decomposed into mean and fluctuating parts. Using this in equation (3.15) yields

$$Nu = \frac{C_1 (\bar{E}_u + e_u)^2}{K \left[C_2 - C_3 (E_T + e_T) \right]} \tag{3.16}$$

The term in the denominator of equation (3.16) can be written as

$$C_2 - C_3(\bar{E}_T + e_T) = (C_2 - C_3\bar{E}_T)\left(1 - \frac{C_3 e_T}{C_2 - C_3\bar{E}_T}\right) \tag{3.17}$$

Substituting equation (3.17) into equation (3.16) gives

$$N_u = \frac{C_1(\bar{E}_u + e_u)^2}{K(C_2 - C_3\bar{E}_T)\left(1 - \frac{C_3 e_T}{C_2 - C_3\bar{E}_T}\right)} \tag{3.18}$$

Expanding the denominator yields

$$N_u \cong \frac{C_1}{K}\frac{(\bar{E}_u + e_u)^2}{(C_2 - C_3\bar{E}_T)}\left(1 + \frac{C_3 e_T}{C_2 - C_3\bar{E}_T}\right) \tag{3.19}$$

By carrying out the indicated operations and averaging, the average Nusse number can be obtained as a function of the voltage moments as

$$Nu \cong \frac{C_1}{K}\left[\frac{\bar{E}_u^2}{C_2 - C_3\bar{E}_T} + \frac{\overline{e_u^2}}{C_2 - C_3\bar{E}_T} + \frac{2C_3\bar{E}_u\overline{e_u e_T}}{(C_2 - C_3\bar{E}_T)} + \frac{C_3\overline{e_u^2 e_T}}{(C_2 - C_3\bar{E}_T)^2}\right] \quad (3$$

This will be reduced further after the other powers of the Nusselt numbe are similarly decomposed.

Consider now $N_u^{\overline{1/2}}$. From equation (3.16)

$$N_u^{1/2} = \left\{\frac{C_1(\bar{E}_u + e_u)^2}{K[C_2 - C_3(\bar{E}_T + e_T)}\right\}^{1/2} \tag{3.2}$$

or

$$N_u^{1/2} = \sqrt{\frac{C_1}{K}}\frac{(\bar{E}_u + e_u)}{\left[(C_2 - C_3\bar{E}_T)\left(1 - \frac{C_3 e_T}{C_2 - C_3\bar{E}_T}\right)\right]^{1/2}} \tag{3.2}$$

Expanding the denominator as before yields

$$N_u^{1/2} \cong \sqrt{\frac{C_1}{K}}\frac{(\bar{E}_u + e_u)}{(C_2 - C_3\bar{E}_T)^{1/2}}\left[1 + \frac{C_3 e_T}{2(C_2 - C_3\bar{E}_T)}\right] \tag{3.2}$$

Averaging equation (3.23) yields

$$\overline{Nu^{1/2}} \cong \sqrt{\frac{C_1}{K}}\left[\frac{\bar{E}_u}{(C_2-C_3\bar{T}_r)^{1/2}} + \frac{C_3\,\overline{e_u e_T}}{2(C_2-C_3\bar{T}_r)^{3/2}}\right] \tag{3.24}$$

In a similar manner, the other two terms, $\overline{Nu^{3/2}}$ and $\overline{Nu^2}$, can also be analyzed and the results are written below:

$$\overline{Nu^{3/2}} \cong \left(\frac{C_1}{K}\right)^{3/2}\left[\frac{\bar{E}_u^3 + 3\bar{E}_u\overline{e_u^2} + \overline{e_u^3}}{(C_2-C_3\bar{T}_r)^{3/2}} + \frac{9C_3\bar{E}_u\overline{e_u^2 e_T} + 9C_3\bar{E}_u^2\overline{e_u e_T} + 3C_3\overline{e_u^3 e_T}}{2(C_2-C_3\bar{T}_r)^{5/2}}\right] \tag{3.25}$$

$$\overline{Nu^2} \cong \left(\frac{C_1}{K}\right)^2\left[\frac{\bar{E}_u^4 + 6\bar{E}_u^2\overline{e_u^2} + 4\bar{E}_u\overline{e_u^3} + \overline{e_u^4}}{(C_2-C_3\bar{T}_r)^2} + \frac{8C_3\bar{E}_u^3\overline{e_u e_T} + 12C_3\bar{E}_u^2\overline{e_u^2 e_T} + 8C_3\bar{E}_u\overline{e_u^3 e_T} + 2C_3\overline{e_u^4 e_T}}{(C_2-C_3\bar{T}_r)^3}\right] \tag{3.26}$$

Comparison of Various Terms

$\overline{N_u^{1/2}}$ Expresion

From equation (3.24) it follows that

$$\overline{Nu^{1/2}} \cong \sqrt{\frac{C_1}{K}}\left[\frac{\bar{E}_u}{(C_2-C_3\bar{T}_r)^{1/2}}\right]\left\{1 + \frac{1}{2}\frac{C_3\,\overline{e_u e_T}}{(C_2-C_3\bar{T}_r)^{1/2}}\cdot\frac{(C_2-C_3\bar{T}_r)^{1/2}}{\bar{E}_u}\right\}$$

For simplicity let the term in brackets be represented as

$$\left\{\quad\right\} = \left\{1 + \frac{B}{A}\right\}$$

We can estimate the magnitude of B/A as follows

$$\frac{B}{A} = \frac{1}{2} \cdot \frac{\overline{e_u e_T}}{\sqrt{\overline{e_u^2}} \cdot \sqrt{\overline{e_T^2}}} \cdot \frac{C_3 \sqrt{\overline{e_T^2}}}{(C_2 - C_3 \bar{E}_T)} \cdot \frac{\sqrt{\overline{e_u^2}}}{\bar{E}_u}$$

or

$$\frac{B}{A} \lesssim \frac{1}{2} \cdot \frac{\sqrt{\overline{t^2}}}{(T_w - T)} \cdot \frac{\sqrt{\overline{e_u^2}}}{\bar{E}_u}$$

since the correlation coefficient is bounded by $\pm$ 1. Assuming an overhea ratio of 1.5 and a temperature, T, of 300°K, we obtain T_w = 1.5 x 300 = 4 The R.M.S. temperature in this experiment is commonly less than 10°K. Therefore

$$\frac{B}{A} \lesssim \left(\frac{1}{2}\right)\left(\frac{10}{150}\right)$$

or

$$\frac{B}{A} \sim \ll 1$$

which is also obvious because the turbulence quantities are smaller magnitude than the mean values. Nonetheless, term B will be kept in further calculations.

$\overline{N_u}$ Expression

Referring to equation (3.20) we can obtain the ratio of the fourth and second terms (D/C) as

$$\frac{D}{C} = \frac{C_3 \overline{e_u^2 e_T}}{(C_2 - C_3 \bar{E}_T)^2} \cdot \frac{(C_2 - C_3 \bar{E}_T)}{\overline{e_u^2}}$$

Using the same argument as above it can be shown that $D/C \lesssim 0.05$

Therefore the triple correlation term will be neglected.

Similarly from equation (3.20) we can compute the ratio of the third and second terms:

$$\frac{\text{3rd term}}{\text{2nd term}} = \frac{2C_3 \bar{E}_U \overline{e_u e_T}}{(C_2 - C_3 \bar{E}_T)^2} \cdot \frac{(C_2 - C_3 \bar{E}_T)}{\overline{e_u^2}} = \frac{4AB}{C} \simeq 1$$

Therefore both the second and third terms must be retained if either is retained.

In general the terms of third or higher order in fluctuating quantities can be shown to be very small as compared to the second order terms. Using the above argument the various $\overline{Nu^n}$ expressions reduce to

$$\overline{Nu^{1/2}} \simeq \left(\frac{C_1}{K}\right)^{1/2} \left[\frac{\bar{E}_u}{(C_2 - C_3 \bar{E}_T)^{1/2}} + \frac{C_3 \overline{e_u e_T}}{2(C_2 - C_3 \bar{E}_T)^{3/2}} \right] \tag{3.27}$$

$$\overline{Nu} \simeq \left(\frac{C_1}{K}\right) \left[\frac{\bar{E}_u^2 + \overline{e_u^2}}{(C_2 - C_3 \bar{E}_T)} + \frac{2C_3 \bar{E}_U \overline{e_u e_T}}{(C_2 - C_3 \bar{E}_T)^2} \right] \tag{3.28}$$

$$\overline{Nu^{3/2}} \simeq \left(\frac{C_1}{K}\right)^{3/2} \left[\frac{\bar{E}_u^3 + 3\bar{E}_u \overline{e_u^2}}{(C_2 - C_3 \bar{E}_T)^{3/2}} + \frac{9C_3 \bar{E}_u^2 \overline{e_u e_T}}{2(C_2 - C_3 \bar{E}_T)^{5/2}} \right] \tag{3.29}$$

$$\overline{Nu^2} \simeq \left(\frac{C_1}{K}\right)^2 \left[\frac{\bar{E}_u^4 + 6\bar{E}_u \overline{e_u^2}}{(C_2 - C_3 \bar{E}_T)^2} + \frac{8C_3 \bar{E}_u^3 \overline{e_u e_T}}{(C_2 - C_3 \bar{E}_T)^3} \right] \tag{3.30}$$

Equations (3.27)-(3.30) can be substituted into the equation (3.11) to yield the final expression for calculating the average Reynolds number and hence the mean velocity.

It is important to note that only two velocity-like moments need be

used $\overline{E_u}$, $\overline{e_u^2}$, and the velocity-temperature voltage correlation $\overline{e_u e_T}$. Unlike the expansion employed by Rao and Brustowski (11) and others which involved neglecting terms of order $(\frac{u}{U})^2$, these expressions do not degenerate as the turbulence intensity increases since $\overline{E}_u$ does not go to zero as does U. Thus this scheme for obtaining the velocity will be valid over the range of flow conditions encountered in this experiment.

R.M.S. Velocity

Subtracting equation (3.11) from (3.3) and squaring yields:

$$u^2 = \left(\frac{\nu}{d}\right)^2 \left[B_1 \left(Nu^{1/2} - \overline{Nu}^{1/2} \right) + B_2 (Nu - \overline{Nu}) + B_3 \left(Nu^{3/2} - \overline{Nu}^{3/2} \right) + B_4 \left(Nu^2 - \overline{Nu}^2 \right) \right]^2 \qquad (3.31)$$

Carrying out the indicated operations yields:

$$u^2 = \left(\frac{\nu}{d}\right)^2 \Big\{ B_1^2 \left(Nu^{1/2} - \overline{Nu}^{1/2} \right)^2 + B_2^2 (Nu - \overline{Nu})^2 + B_3^2 \left(Nu^{3/2} - \overline{Nu}^{3/2} \right) + B_4^2 \left(Nu^2 - \overline{Nu}^2 \right) +$$

$$2B_1 \left(Nu^{1/2} - \overline{Nu}^{1/2} \right) \left[B_2 (Nu - \overline{Nu}) + B_3 \left(Nu^{3/2} - \overline{Nu}^{3/2} \right) + B_4 \left(Nu^2 - \overline{Nu}^2 \right) \right]$$

$$2B_2 (Nu - \overline{Nu}) \left[B_3 \left(Nu^{3/2} - \overline{Nu}^{3/2} \right) + B_4 \left(Nu^2 - \overline{Nu}^2 \right) \right] +$$

$$2B_3 \left(Nu^{3/2} - \overline{Nu}^{3/2} \right) \left[B_4 \left(Nu^2 - \overline{Nu}^2 \right) \right] \Big\} \qquad (3.32)$$

Consider the following term

$$\left(Nu^{1/2} - \overline{Nu}^{1/2} \right)^2 = Nu + \left(\overline{Nu}^{1/2} \right)^2 - 2 Nu^{1/2} \overline{Nu}^{1/2}$$

After averaging it reduces to

$$\overline{Nu} - \left(\overline{Nu}^{1/2} \right)^2$$

Also consider the term

$$2B_1\left(Nu^{1/2} - \overline{Nu^{1/2}}\right) B_2 \left(Nu - \overline{Nu}\right)$$

Simplifying and averaging yields

$$2B_1B_2\left(\overline{Nu^{3/2}} - \overline{Nu^{1/2}}\,\overline{Nu}\right)$$

Using the same type of analysis for each term in equation (3.32) yields an expression for the R.M.S. velocity as:

$$\begin{aligned}\sqrt{\overline{u^2}} = \frac{\nu}{d}\Big[& B_1^2\left(\overline{Nu} - \overline{Nu^{1/2}}^2\right) + B_2^2\left(\overline{Nu^2} - \overline{Nu}^2\right) + \\ & B_3^2\left(\overline{Nu^3} - \overline{Nu^{3/2}}^2\right) + B_4^2\left(\overline{Nu^4} - \overline{Nu^2}^2\right) + \\ & 2B_1B_2\left(\overline{Nu^{3/2}} - \overline{Nu^{1/2}}\,\overline{Nu}\right) + 2B_1B_3\left(\overline{Nu^2} - \overline{Nu^{1/2}}\,\overline{Nu^{3/2}}\right) + \\ & 2B_1B_4\left(\overline{Nu^{3/2}} - \overline{Nu^{1/2}}\,\overline{Nu^2}\right) + 2B_2B_3\left(\overline{Nu^{5/2}} - \overline{Nu}\,\overline{Nu^{3/2}}\right) + \\ & 2B_2B_4\left(\overline{Nu^3} - \overline{Nu}\cdot\overline{Nu^2}\right) + 2B_3B_4\left(\overline{Nu^{7/2}} - \overline{Nu^{3/2}}\,\overline{Nu^2}\right)\Big]\end{aligned} \tag{3.33}$$

$\overline{Nu^{1/2}}$, $\overline{Nu}$, $\overline{Nu^{3/2}}$, $\overline{Nu^2}$ are already calculated in equations (3.27)-(3.30) whereas the other Nu expressions can be derived along the same lines; the final results after neglecting smaller terms are written below.

$$\overline{Nu^{5/2}} \cong \left(\frac{C_1}{K}\right)^{5/2}\left[\frac{\bar{E}_U^5 + 10\bar{E}_U^3\,\overline{e_u^2}}{(C_2 - C_3\bar{E}_T)^{5/2}} + \frac{25\,C_3\,\bar{E}_U^4\,\overline{e_u e_T}}{2(C_2 - C_3\bar{E}_T)^{7/2}}\right] \tag{3.34}$$

$$\overline{Nu^3} \cong \left(\frac{C_1}{K}\right)^3\left[\frac{\bar{E}_U^6 + 15\bar{E}_U^4\,\overline{e_u^2}}{(C_2 - C_3\bar{E}_T)^3} + \frac{18\,C_3\,\bar{E}_U^5\,\overline{e_u e_T}}{(C_2 - C_3\bar{E}_T)^4}\right] \tag{3.35}$$

$$\overline{Nu^{7/2}} \cong \left(\frac{C_1}{K}\right)^{7/2}\left[\frac{\bar{E}_U^7 + 21\bar{E}_U^5\overline{e_U^2}}{(C_2 - C_3\bar{E}_T)^{7/2}} + \frac{49\,C_3\bar{E}_U^6\overline{e_U e_T}}{2(C_2 - C_3\bar{E}_T)^{9/2}}\right] \tag{3.36}$$

$$\overline{Nu^4} \cong \left(\frac{C_1}{K}\right)^4\left[\frac{\bar{E}_U^8 + 28\bar{E}_U^6\overline{e_U^2}}{(C_2 - C_3\bar{E}_T)^4} + \frac{56\,C_3\bar{E}_U^7\overline{e_U e_T}}{(C_2 - C_3\bar{E}_T)^5}\right] \tag{3.37}$$

Velocity-Temperature Correlation

Subtract equation (3.8) from equation (3.4) to get

$$t = A_2 e_T \tag{3.38}$$

Similarly subtract equation (3.11) from (3.3) to get

$$u = \frac{\nu}{d}\left[B_1(Nu^{1/2} - \overline{Nu^{1/2}}) + B_2(Nu - \overline{Nu}) + B_3(Nu^{3/2} - \overline{Nu^{3/2}}) + B_4(Nu^2 - \overline{Nu^2})\right] \tag{3.39}$$

Multiplying equations (3.38) and (3.39) and averaging yields

$$\overline{ut} = \frac{A_2\nu}{d}\left[B_1\overline{Nu^{1/2}e_T} + B_2\overline{Nu\,e_T} + B_3\overline{Nu^{3/2}e_T} + B_4\overline{Nu^2 e_T}\right] \tag{3.40}$$

Consider each term individually on the right side of equation (3.4). Multiplying equation (3.23) by e_T, averaging and neglecting third order terms, yields

$$\overline{Nu^{1/2}e_T} \cong \left(\frac{C_1}{K}\right)^{1/2}\left[\frac{\overline{e_U e_T}}{(C_2 - C_3\bar{E}_T)^{1/2}} + \frac{C_3\bar{E}_U\overline{e_T^2}}{2(C_2 - C_3\bar{E}_T)^{3/2}}\right] \tag{3.41}$$

Performing the same type of algebra for other terms leads to the results written below

$$\overline{Nu\, e_T} \cong \frac{C_1}{K}\left[\frac{2\bar{E}_u \overline{e_u e_T}}{(C_2 - C_3\bar{E}_T)} + \frac{C_3 \bar{E}_u^2 \overline{e_T^2}}{(C_2 - C_3\bar{E}_T)^2}\right] \tag{3.42}$$

$$\overline{Nu^{3/2} e_T} \cong \left(\frac{C_1}{K}\right)^{3/2}\left[\frac{3\bar{E}_u^2 \overline{e_u e_T}}{(C_2 - C_3\bar{E}_T)^{3/2}} + \frac{3C_3\bar{E}_u^3 \overline{e_T^2}}{2(C_2 - C_3\bar{E}_T)^{5/2}}\right] \tag{3.43}$$

$$\overline{Nu^2 e_T} \cong \left(\frac{C_1}{K}\right)^2\left[\frac{4\bar{E}_u^2 \overline{e_u e_T}}{(C_2 - C_3\bar{E}_T)^2} + \frac{2C_3\bar{E}_u^3 \overline{e_T^2}}{(C_2 - C_3\bar{E}_T)^3}\right] \tag{3.44}$$

By substituting equations (3.41)-(3.44) into the equation (3.40) the velocity-temperature correlation can be obtained.

Summary

It is clear from the above that all of the moments of interest in this experiment can be obtained by measuring only the second order moments of the velocity and temperature signals, and their correlations.

The calculated and measured quantities are summarized below

Calculated	Measured
$\bar{U}$	$\bar{E}_u$
$\overline{u^2}$	$\overline{e_u^2}$
$\overline{\Delta T}$	$\bar{E}_T$
$\overline{t^2}$	$\overline{e_T^2}$
$\overline{ut}$	$\overline{e_u e_T}$

Each of the terms on the left is uniquely determined by a subset of the terms in the right, the coefficients depending on the calibration law.

Chapter 4 - Experimental Results and Discussions

4.1 Results

The measurements were taken at three different vertical locations of 1.0, 1.5, 2.0 meters which when normalized by the source diameter of 6.35 cm correspond to an x/D of 15.74, 23.62 and 31.49 respectively. The mean axial velocity and the mean temperature difference (between the plume and the ambient) normalized by the similarity variables were plotted against the dimensionless distance from the center of the plume. The profiles are shown in figures (4-1) and (4-2) respectively.

The buoyancy parameter was calculated by integrating the heat flux at the source using

$$F_o = 2\pi \int_0^\infty g\, U \frac{\Delta\rho}{\rho_\infty} r\, dr \qquad (4.1)$$

Using the fact that the profiles at the exit are uniform (i.e. the exit velocity and density of air are constant across the exit), equation (4.1) reduces to

$$F_o = 2\pi g \frac{\Delta\rho}{\rho_\infty} Q_e \qquad (4.2)$$

where Q_e is the volumetric flow-rate.

The density of air at the various temperatures of interest is given in the following table

TABLE I

Location	Temperature (°K)	Density (KG/m^3)
Inlet air	290	1.218
Ambient	295	1.197
Source	566	0.6234

The conservation of mass gives

$$\rho Q = \rho_e Q_e \qquad (4.3)$$

where ρ and Q are the density and volumetric flowrate measured by the

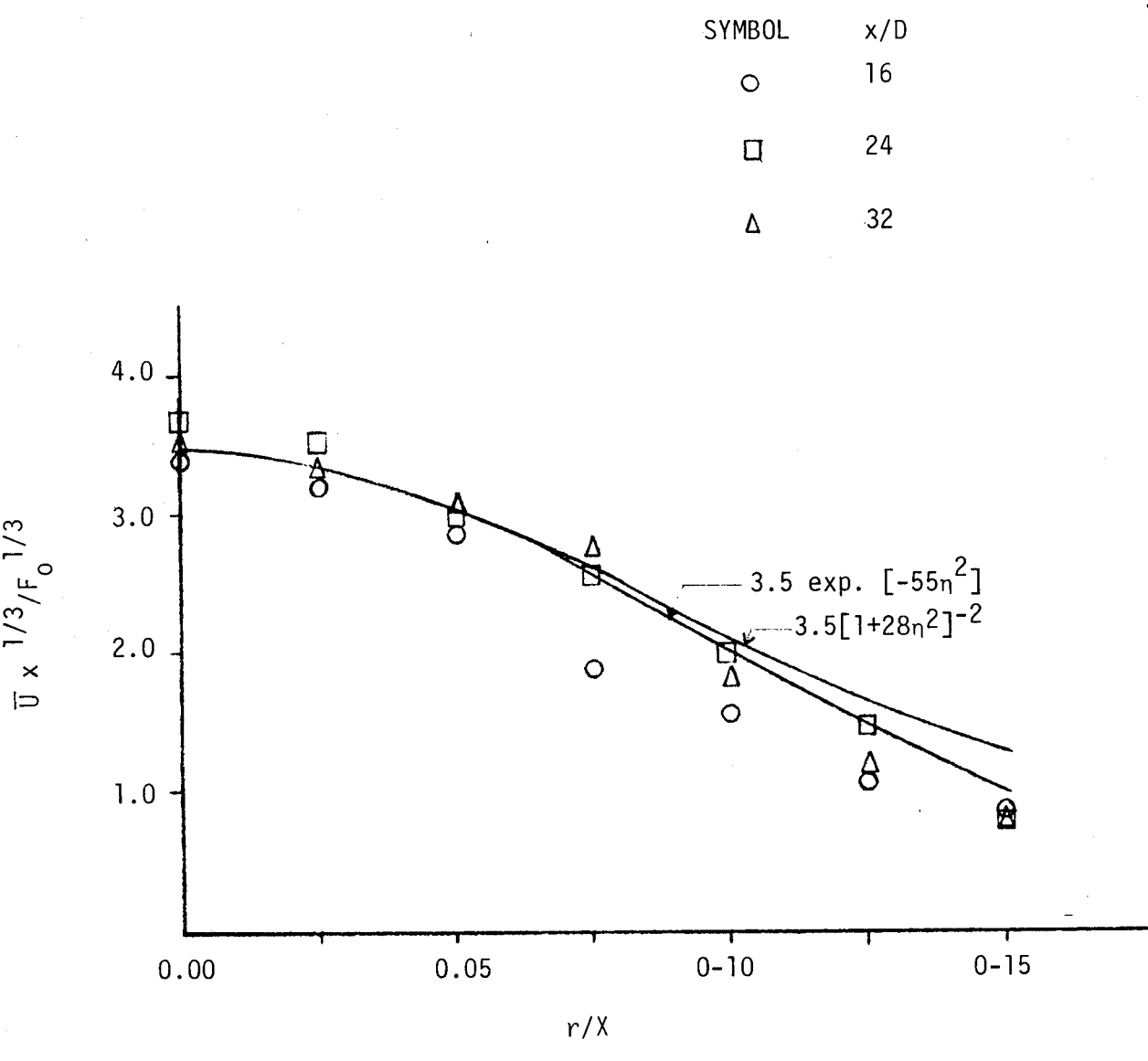

Figure (4-1) Mean Axial Velocity

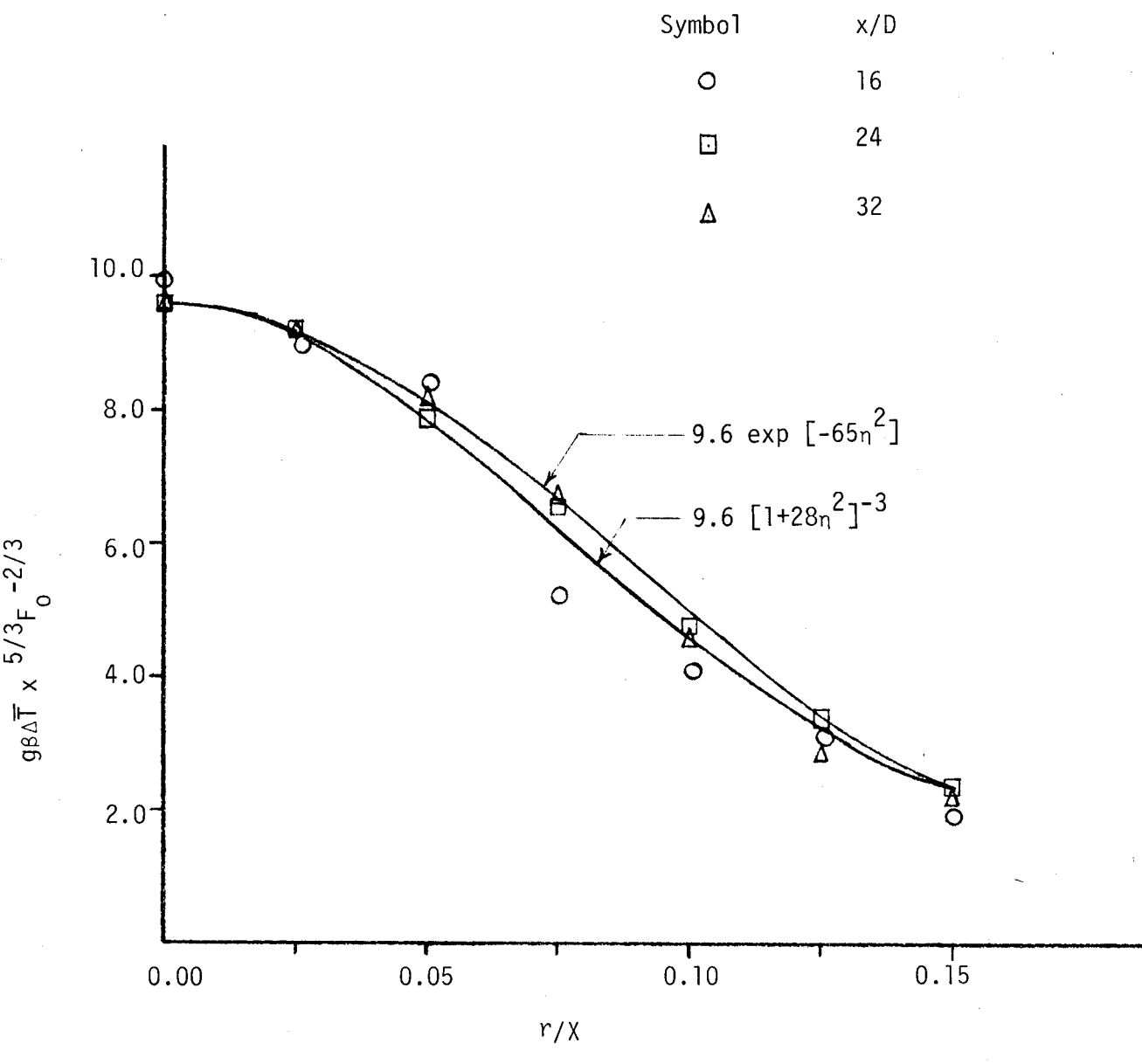

Figure (4-2) Mean Temperature

rotometer and the subscript e stands for the exit conditions.

In this experiment

$$Q = 150 \text{ ft}^3/\text{hr}$$
$$= 1.18 \times 10^{-3} \text{ m}^3/\text{sec}.$$

From equation (4.3)

$$Q_e = 2.27 \times 10^{-3} \text{ m}^3/\text{sec}.$$

Substituting the value of Q_e in equation (4.2) we get $F_o = .01067 \text{ m}^4/\text{sec}^3$

The profiles of R.M.S. velocity and temperature fluctuations normali with the mean velocity and temperature difference at the centerline are shown in figures (4-3) and (4-4) respectively.

The velocity temperature correlation was measured and converted to the correlation coefficient using the measured R.M.S. values. The result are plotted against dimensionless radius in figure (4-5).

The rate at which buoyancy crosses any normalized plane can be obtai by integrating the total heat flux across the various axial sections. Since the plume is unstratified, this should be the same at all vertical locations and equal to F_o, the rate at which buoyancy is added at the sou It was observed that there was a decrease in the buoyancy of about 2% at 4% at 1.5 m and 7% at 2 m due to slight stratification in the room. The normalized buoyancy profile including the contribution from the turbulent heat transport is shown in the figure (4-6).

Throughout the investigation, the ambient temperature was continuous monitored. In fact it was during this investigation that the stratificat problem reported by Beuther (4) was discovered. That the modifications discussed earlier were successful in eliminating the stratification is illustrated by figure (4-7) which shows the temperature variation over th course of a single experiment. The slight gradient over the range of

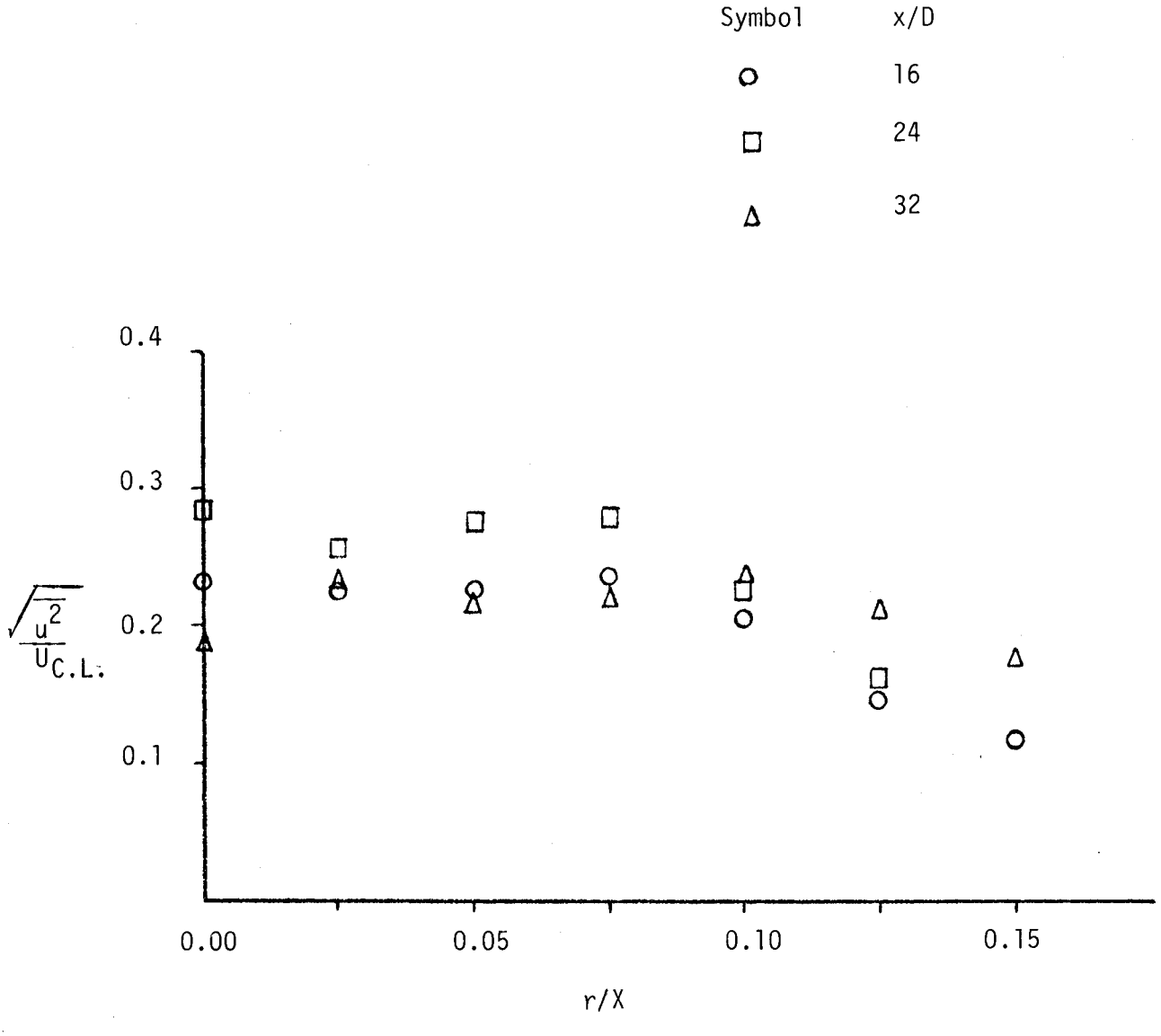

Figure (4-3) Intensity of Axial Velocity Fluctuations

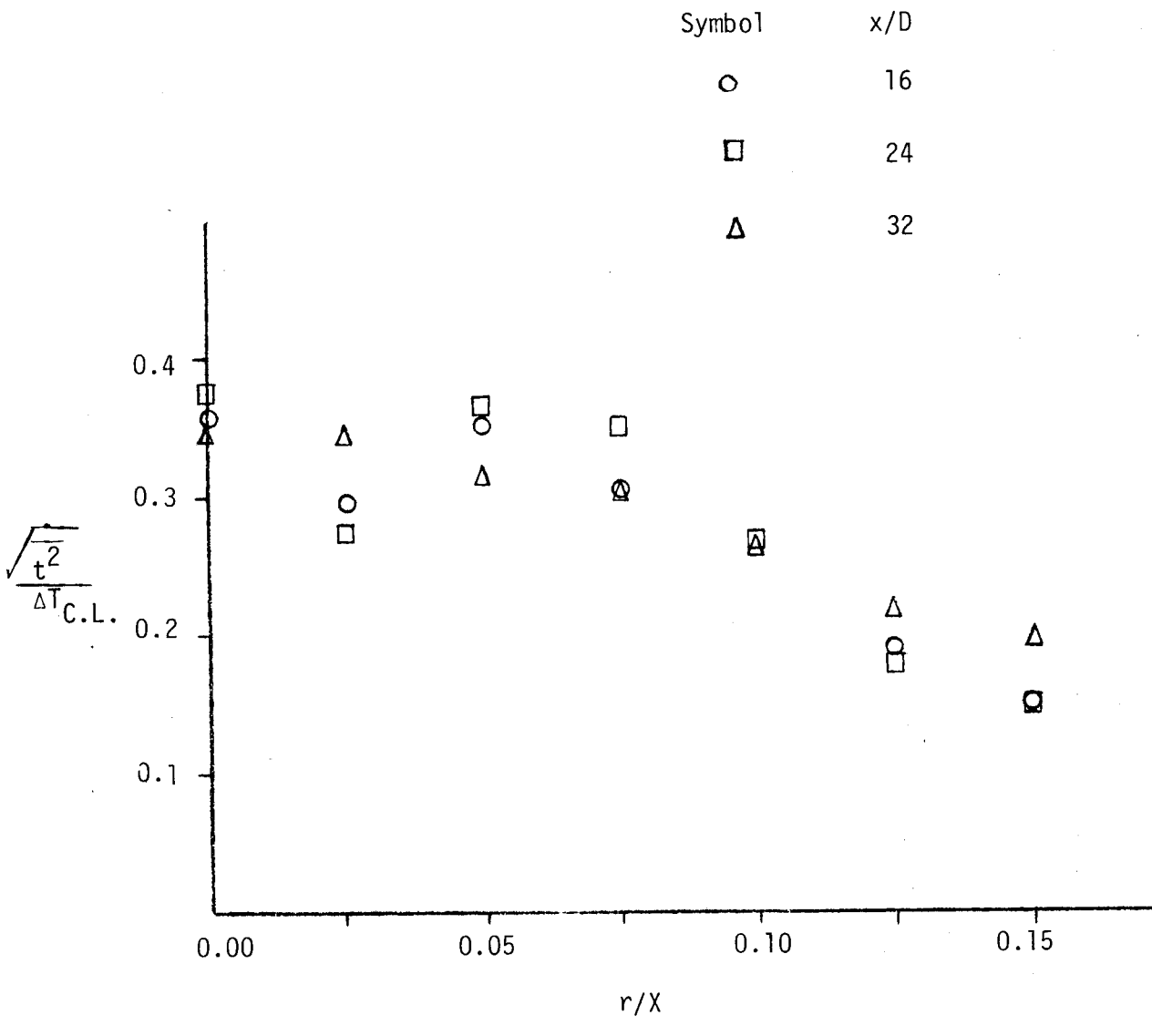

Figure (4-4) Intensity of Temperature Fluctuations

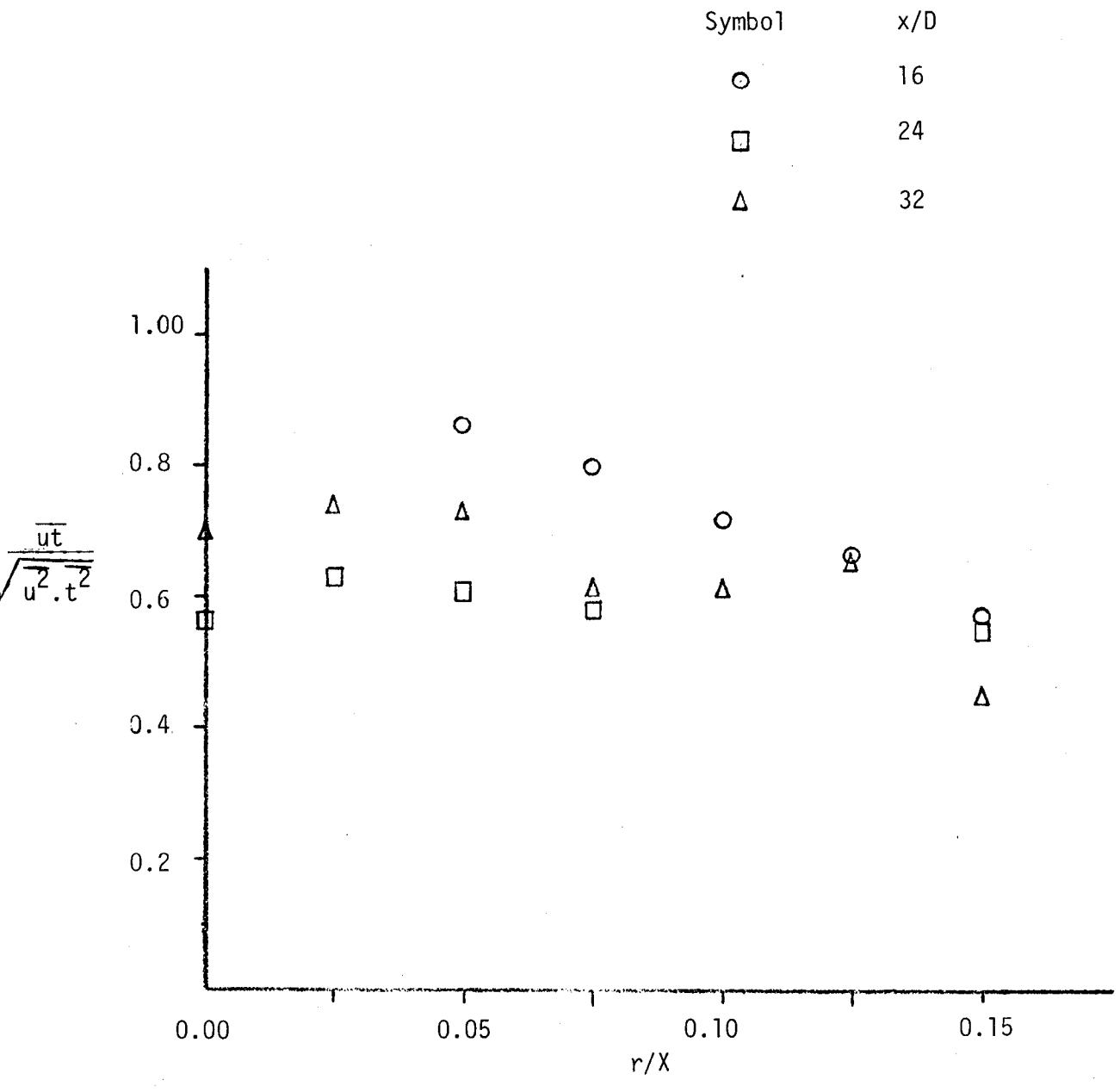

Figure (4-5) The Velocity-Temperature Correlation Coefficient

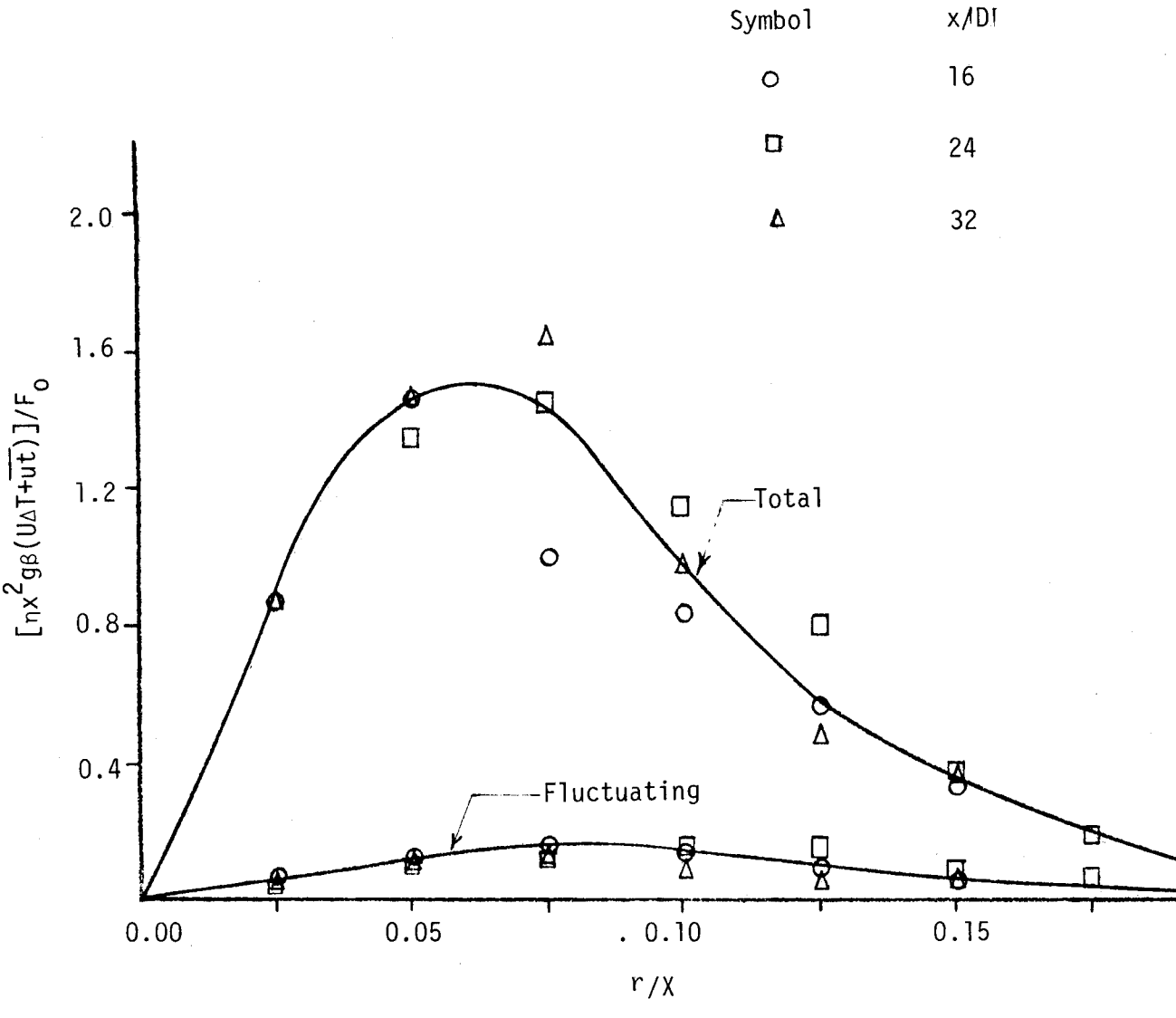

Figure (4-6) Integrand of Buoyancy Integral

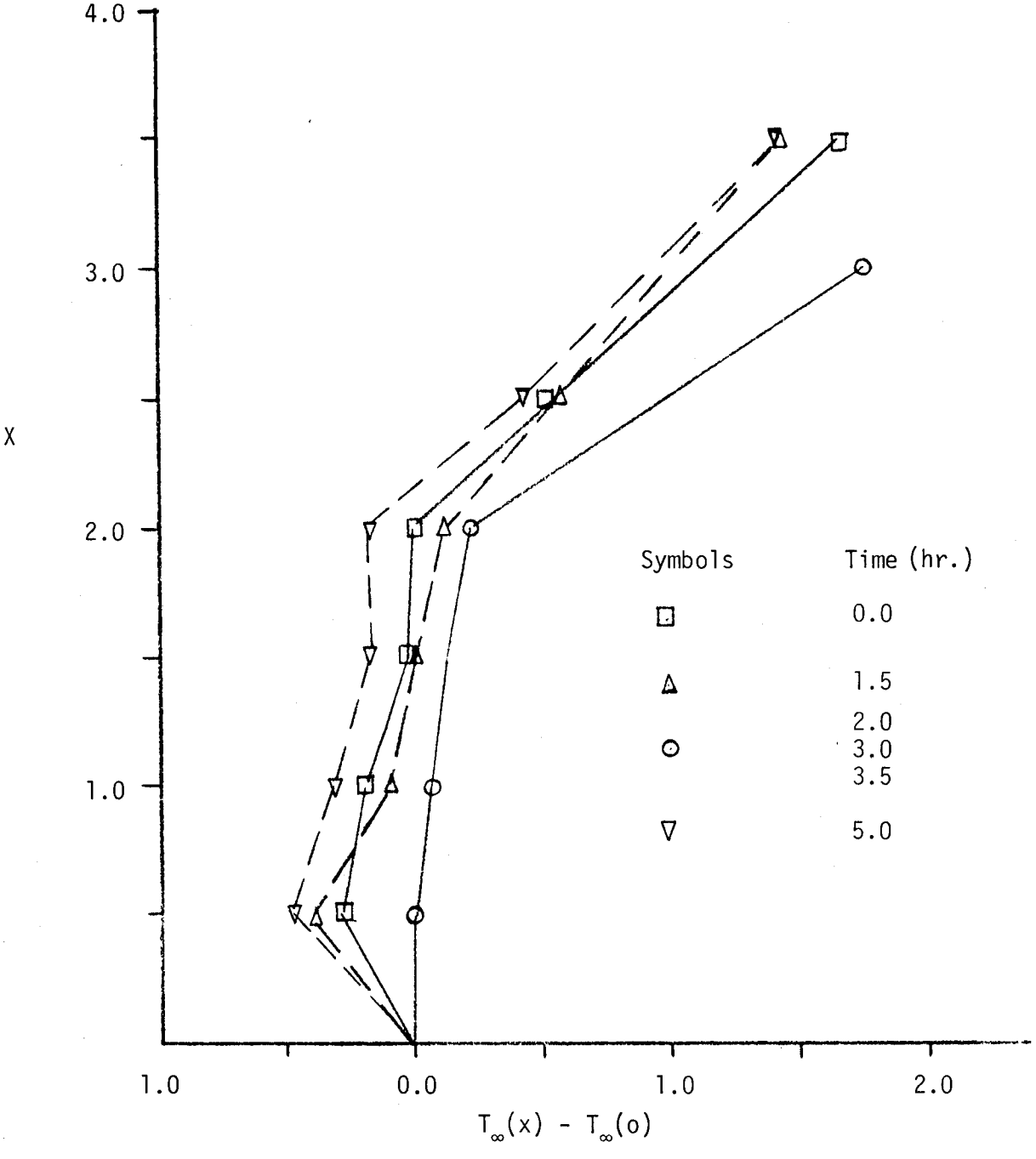

Figure (4-7) Ambient Temperature

measurement ($\leq$ 2m) is consistent with the slight decrease in the buoyancy integral with height.

4.2 Discussion

Baker (1) concluded that if the parameter ξ (forced length scale was ≤ 1, the flow was dominated by the momentum and would behave like a jet. ξ is defined as $\xi = \frac{x}{L}$ where $L = \frac{M^{3/4}}{F_o^{1/2}}$. If the $\xi \geq 10$, the flow is dominated by the buoyancy and exhibits the properties of plume-like flows.

The criterion was applied to check the behavior of the flow at the locations of interest for the present experiment. The rate at which momentum is added at the source is calculated as

$$M = 2\pi \int_0^{r_0} U^2 r \, dr$$

$$= A U_o^2$$

$$= (3.167 \times 10^{-3})(0.717)^2$$

$$= 1.628 \times 10^{-3} \text{ m}^4/\text{sec}^2$$

and the rate at which buoyancy is added at the source is

$$F_o = 0.01067 \text{ m}^4/\text{sec}^3$$

Thus the length scale L is determined as

$$L = \frac{M^{3/4}}{F_o^{1/2}}$$

$$= 0.07845 \text{ m}$$

Thus $\xi = 10$ corresponds to an axial distance from the source of

$$x = \xi L$$

$$\cong 0.78 \text{ m}$$

Under the source conditions specified above and Baker's criterion, the flow behaves like a plume if the axial distance for measurements from the source is greater than 0.78 m. Such was the case in this experiment since the probe was at least 1 meter high from the source

Two different forms of curves were fitted to the mean velocity and temperature data shown in figures (4-1) and (4-2) respectively. One of those was the exponential type of fit used by George et al. (6), of the form of

$$U(x/F_0)^{1/3} = 3.5 \exp.(-55\eta^2)$$

and

$$g\beta\Delta T\left(x^5/F_0^2\right)^{1/3} = 9.6 \exp.(-65\eta^2)$$

The second was of the form of Yih's analytical solutions

$$f(\eta) = \frac{f_1}{(1+A\eta^2)^2}$$

and

$$p(\eta) = \frac{p_1}{(1+A\eta^2)^3}$$

where

$$A = 2.8$$

$$f_1 = 3.5$$

$$b = 9.6$$

It is obvious from the measurements that the profiles are self-preserving. The centerline value, 3.5, for the normalized mean velocity is in between the value 3.4 predicted by George et al. and the value 3.6 measured by Beuther et al. The mean temperature centerline value is 9.6 which is close to the value 9.5 measured by Beuther et al. and a little higher than the value 9.1 found by George et al. The two mean profiles have nearly the same shape as that reported by George et al. (6) and thus lend support to their results.

The R.M.S. velocity and temperature fluctuations are shown in figure (4-3) and (4-4). The intensity of velocity fluctuations at the centerlin is about 24% of the centerline mean velocity, which is lower than the values of 0.26 and 0.28 predicted by Beuther et al. and George et al. At this point, the reasons for the dip of the curve at $\eta = 0.025$ are not known; this will be explored in subsequent investigations but is probably just an error in the measurement. The R.M.S. temperature at the centerli is about 36% of the mean centerline temperature difference as compared to the values 40% and 36% referred to by George et al. and Beuther et al. respectively.

The correlation coefficient is about 0.7 and remains nearly constant across the flow. George et al. found this number equal to 0.67 while Beuther et al. obtained 0.55. While these measurements appear to support the earlier results, the difference might be attributable to the

fact that unlike this investigation and that of George et al., Beuther used an x-wire. This possibility will have to be explored later.

In a flow dominated by buoyancy, the temperature fluctuations generate velocity fluctuations and consequently the high correlation coefficient is reasonable. The high value of correlation coefficient is responsible for about 13% of the heat flux being carried by the turbulence, which in any case cannot be ignored.

A disappointment in this experiment is the large scatter in the data, which is present in almost all the profiles. One possible reason may be due to the data analysis technique which involves subtraction of nearly equal quantities in the data conversion equations. A very slight error in these big numbers results in an appreciable change in the quantity being estimated. The uncertainty in the measured R.M.S. voltages appears to be the primary source of the scatter and it contributes to both mean and R.M.S. quantities. While this scatter could be reduced by longer integration times (20 minute averages were used) there would be difficulties in maintaining stable conditions in the room since this is already a lengthy experiment of about ten hours duration.

Chapter 5 - Summary and Conclusions

The purpose of this thesis was to investigate the turbulent buoyant plume under neutrally stable ambient conditions. To check this condition the temperature at various heights was continuously monitored by thermocouples during the experiment. To find the mean and fluctuating velocities and temperatures, a parallel wire probe was used, one operated at constant temperature and the other operated at constant current. The probe was positioned in the flow in such a way to avoid interference of one wire with the wake of the other.

A polynominal of the form

$$Re = B_0 + B_1 Nu^{1/2} + B_2 Nu + B_3 Nu^{3/2} + B_4 Nu^2$$

was used for the velocity calibration data.

A linear law of the form of

$$T = A_0 + A_2 E_T$$

was used for the temperature calibration.

To unravel the raw data, the instantaneous values of temperature and velocity-like signals were substituted in the calibration equation, decomposed into the mean and fluctuating components, and the whole equation was then averaged to get the mean velocity and temperature. The mean equations were then subtracted from the full equations, squared and averaged to obtain the relationship for R.M.S. quantities. Finally to find the correlation between velocity and temperature, the fluctuating components of instantaneous values were multiplied and averaged. Only second order moments of the velocity and temperature voltage signals and their correlation were necessary to compute all the second order statistics, the high order contributions being negligible. Since only ratios of fluctuating voltages to mean voltages were encountered and since the mean voltages do not go to zero with the

mean velocity, the technique is applicable to even high intensity turbulent flows.

While it was not possible to achieve absolutely uniform ambient conditions, only a very slight stratification in the environment was observed and this was reflected in the relative constancy of the buoyancy integral. The results are much closer to those of George et al.(6) than to those of Beuther (5) and confirm that stratification has influenced the latter.

There is significant scatter in the data in almost all the profiles. This was attributed to the fluctuations in thw R.M.S. signals recorded which contribute to both the mean and turbulent quantities. It is therefore suggested that if the present technique is to be used effectively, the uncertainty in the recorded signals must be removed by increasing the averaging time.

References

1. Baker, C.B., *An Analysis of the Turbulent Buoyant Jet.* A Ph.D. dissertation submitted to the Graduate School of State University of Pennsylvania, Feb. 1980.

2. Baker, C.B., D.B. Taulbee, W.K. George, *Eddy Viscosity Calculations of Turbulent Buoyant Plumes.* Joint ASME/AIChE 18th National Heat Transfer Conference, San Diego, Ca. 1979.

3. Batchelor, G.K., *Heat Convection and Buoyancy Effects in Fluids,* Q. Jl. R. Met. Soc. 80, 334-358 (1954).

4. Beuther, P. D.,*Experimental Investigation of the Axisymmetric Turbulent Buoyant Plume.* Ph.D. dissertation submitted to the Graduate School of State University of New York at Buffalo, 1980.

5. Beuther, P.D., Capp, S.P., George, W.K., *Momentum and Temperature Balance Measurements in an Axisymmetric Turbulent Plume.* Joint ASME/AIChE 18th National Heat Transfer Conference, San Diego, Ca. 19

6. George, W.K., R.L. Alpert and F. Tamanini, *Turbulence Measurements in an Axisymmetric Buoyant Plume,* Int. J. Heat Mass Trans. V. 20, 1145-1154, 1977.

7. Hamilton, C.M., George, W.K.,*Eddy Viscosity Calaculations for Turbul Buoyant Plumes.* Bull. Am. Phys. Soc., Series II, Vol. 21, No. 10 1225, 1976.

8. Madni, I.K. and R.H. Pletcher., *Predictions of Turbulent Forced Plum Issuing Vertically into Stratified or Uniform Ambients.* Trans. ASME J. Heat Transfer, 99-104, 1977.

9. Morton, B.R., G.I. Taylor and D.S. Turner, *Turbulent Gravitational Convection from Maintained and Instantaneous Source.* Proc. R. Soc. 234A, 1-23, 1956.

10. Nakagome, H. and M. Hirata, *The Structure of Turbulent Diffusion in an Axisymmetric Thermal Plume*, 9th Int. Conf. for Heat and Mass Trans. Inter. Seminar, Spalding D., ed. Vol. 1, 361-372, Hemisphere Publishing Corp. Dubrovnik, Yugoslavia. 1976.

11. Rao, V.K. and Brzuztowshi, T.A., *Preliminary Hot-wire Measurements in Free Convection Zones over Model Fires*. Combust. Sci. Tech. 1, 171-180, 1969.

12. Rouse, H., C.S. Yih and H.W. Humphreys, *Gravitational Convection from a Boundary Source*. Tellus 4, 201, 1952.

13. Schmidt, W.Z.,*Turbulent Propagation of a Stream of Heated Air*. Z. Agnew. Math. Mech. 21, 265-351, 1941.

14. Taylor, G.I.,*Dynamics of a Mass of Hot Gas Rising in Air*. U.S. Atomic Energy Commission, MDDC, 919, LADC 276, 1945.

15. Yih, C.S.,*Turbulent Buoyant Plumes*. The Physics of Fluids, 20, 8, 1234-1237 (1977).

16. Zel'dovich, Ya.B., *Limiting Laws for Turbulent Flows in Free Convection*. Zh. Eksp. Teoret. Fiz. 7 (12), 1463, 1937.